PTEP

Prog. Theor. Exp. Phys. **2022** 013B08(25 pages)
DOI: 10.1093/ptep/ptab149

Condensates, massive gauge fields, and confinement in the SU(3) gauge theory

Hirohumi Sawayanagi

National Institute of Technology, Kushiro College, Kushiro, 084-0916, Japan
*E-mail: sawa@kushiro-ct.ac.jp

Received August 24, 2021; Revised November 6, 2021; Accepted December 1, 2021; Published December 3, 2021

SU(3) gauge theory in the nonlinear gauge of the Curci–Ferrari type is studied. In the low-energy region, ghost condensation and subsequent gauge field condensation can happen. The latter condensation makes classical gauge fields massive. If the color electric potential with a string is chosen as the classical gauge field, it produces the static potential with the linear potential. We apply this static potential to the three-quark system, and show, differently from the Y-type potential, that infrared divergence remains in the Δ-type potential. The color electric flux is also studied, showing that a current which plays the role of the magnetic current appears

Subject Index B03

1. Introduction

In the dual superconductor picture of quark confinement, it is expected that monopole condensation appears in the low-energy region. This condensation produces a mass of gauge fields, and confinement happens. To describe this scenario, the dual Ginzburg–Landau model has been considered (see, e.g., Ref. [1]).

Based on the SU(2) gauge theory in a nonlinear gauge, we considered another possibility to give a mass for gauge fields [2]. In the low-energy region below $\Lambda_{\rm QCD}$, which is the QCD scale parameter, ghost condensation happens. Although this condensation gives rise to a tachyonic gluon mass, a gauge field condensate $\langle A^{+\mu}A^{-}_{\mu}\rangle$ can remove the tachyonic mass. If there is a classical U(1) gauge field, this classical field becomes massive by this condensate.

In Ref. [3], referring to Zwanziger's formalism [4], the electric potential and its dual potential were introduced as a classical field. Due to the string structure of these classical fields, the linear potential was obtained.

In this paper we extend the previous approach to the SU(3) case. In the next section, ghost condensation is studied at the one-loop level. In Sect. 3, under ghost condensation, tachyonic gluon masses and the gluon condensates $\langle A^{a\mu}A^{a}_{\mu}\rangle$ are calculated in the low-momentum limit. The Lagrangian of the massive classical gauge fields is also presented. In Sect. 4, the color electric potential and its dual potential are introduced as classical fields, and the static potential between two charges is calculated. Using the result of Sect. 4, the mesonic potential and the baryonic potential are discussed in Sect. 5. Differently from the dual Ginzburg–Landau model, there is no magnetic current originally. Maxwell's equations in the present model are studied in Sect. 6. The behavior of the color flux tube is also considered. Section 7 is devoted to summary and comment. In Appendix A, the relation between the ghost condensation and

Funded by SCOAP[3]
Funded by SCOAP[3]

$\Lambda_{\rm QCD}$ is derived. Tachyonic gluon masses are calculated in Appendix B. To make the article self-contained, an example of the electric potential and its dual potential for a color charge is presented in Appendix C. In Appendix D, the static potential between two charges is calculated in detail. Based on a phenomenological Lagrangian for order parameters, the type of the dual superconductivity in the present model is considered in Appendix E.

2. Ghost condensation

2.1 *Notation*

We consider the SU(3) gauge theory with structure constants f_{abc} in the Minkowski space. The Lagrangian in the nonlinear gauge of the Curci–Ferrari type [5] is given by [6]

$$\mathcal{L} = \mathcal{L}_{\rm inv} + \mathcal{L}_{\rm NL}, \qquad \mathcal{L}_{\rm inv} = -\frac{1}{4}F^a_{\mu\nu}F^{a\mu\nu},$$
$$\mathcal{L}_{\rm NL} = B^a\partial_\mu A^{a\mu} + i\bar{c}^a(\partial_\mu D^\mu c)^a + \frac{\alpha_1}{2}B^aB^a + \frac{\alpha_2}{2}\bar{B}^a\bar{B}^a - B^aw^a \qquad (a = 1, \ldots, 8),$$

where B^a is the Nakanishi–Lautrup field, c ($\bar{c}$) is the ghost (antighost), $\bar{B}^a = -B^a + igf_{abc}\bar{c}^bc^c$, α_1 and α_2 are gauge parameters, and w^a is a constant to keep the Becchi–Rouet–Stora symmetry. The Lagrangian $\mathcal{L}_{\rm NL}$ is rewritten as

$$\mathcal{L}_\varphi = \frac{\alpha_1}{2}B^aB^a + B^a(\partial_\mu A^{a\mu} + \varphi^a - w^a) + i\bar{c}^a\left[(\partial_\mu D^\mu)^{ac} + gf_{abc}\varphi^b\right]c^c - \frac{\varphi^a\varphi^a}{2\alpha_2},$$

where the auxiliary field φ^a represents $-\alpha_2\bar{B}^a$.

Let us expand the gauge field A_μ as

$$A_\mu = A^a_\mu\frac{\lambda^a}{2} = \vec{A}_\mu\cdot\vec{H} + \sum_{\alpha=1}^{3}\left(W^{-\alpha}_\mu E_\alpha + W^\alpha_\mu E_{-\alpha}\right), \tag{1}$$

where the diagonal components are

$$\vec{A}_\mu = (A^3_\mu, A^8_\mu), \qquad \vec{H} = (H^3, H^8) = \left(\frac{\lambda^3}{2}, \frac{\lambda^8}{2}\right),$$

and $\vec{A}_\mu\cdot\vec{H} = \sum_{A=3,8}A^A_\mu H^A = A^3_\mu H^3 + A^8_\mu H^8$. The off-diagonal components are given by

$$W^{\pm1}_\mu = \tfrac{1}{\sqrt{2}}\left(A^1_\mu \pm iA^2_\mu\right), \qquad W^{\pm2}_\mu = \tfrac{1}{\sqrt{2}}\left(A^4_\mu \mp iA^5_\mu\right), \qquad W^{\pm3}_\mu = \tfrac{1}{\sqrt{2}}\left(A^6_\mu \pm iA^7_\mu\right),$$
$$E_{\pm1} = \tfrac{1}{2\sqrt{2}}(\lambda^1 \pm i\lambda^2), \qquad E_{\pm2} = \tfrac{1}{2\sqrt{2}}(\lambda^4 \mp i\lambda^5), \qquad E_{\pm3} = \tfrac{1}{2\sqrt{2}}(\lambda^6 \pm i\lambda^7).$$

Using the root vectors of the SU(3) group

$$\vec{\epsilon}_1 = (1, 0), \qquad \vec{\epsilon}_2 = \left(\frac{-1}{2}, \frac{-\sqrt{3}}{2}\right), \qquad \vec{\epsilon}_3 = \left(\frac{-1}{2}, \frac{\sqrt{3}}{2}\right), \tag{2}$$

the above matrices satisfy

$$[\vec{H}, E_{\pm\alpha}] = \pm\vec{\epsilon}_\alpha E_{\pm\alpha}, \qquad [E_\alpha, E_{-\alpha}] = \vec{\epsilon}_\alpha\cdot\vec{H}, \qquad [E_{\pm\alpha}, E_{\pm\beta}] = \frac{\mp1}{\sqrt{2}}\varepsilon_{\alpha\beta\gamma}E_{\mp\gamma}$$

and

$$\mathrm{tr}\left(H^AH^B\right) = \frac{\delta^{AB}}{2}, \qquad \mathrm{tr}\left(E_\alpha E_{-\beta}\right) = \frac{\delta^{\alpha\beta}}{2}.$$

In the same way, c and $\bar{c}$ are expressed as

$$c = \vec{c}\cdot\vec{H} + \sum_{\alpha=1}^{3}\left(C^{-\alpha}E_\alpha + C^\alpha E_{-\alpha}\right), \qquad \bar{c} = \vec{\bar{c}}\cdot\vec{H} + \sum_{\alpha=1}^{3}\left(\bar{C}^{-\alpha}E_\alpha + \bar{C}^\alpha E_{-\alpha}\right), \tag{3}$$

where

$$C^{\pm 1} = \frac{1}{\sqrt{2}}\left(c^1 \pm ic^2\right), \qquad C^{\pm 2} = \frac{1}{\sqrt{2}}\left(c^4 \mp ic^5\right), \qquad C^{\pm 3} = \frac{1}{\sqrt{2}}\left(c^6 \pm ic^7\right),$$

and $\bar{C}^{\pm\alpha}$ ($\alpha = 1, 2, 3$) are defined as well.

2.2 *Ghost condensation*

To obtain the one-loop effective potential of φ^A, we diagonalize $\varphi^a \frac{\lambda^a}{2}$ as $\vec{\varphi}\cdot\vec{H}$. Then, using the expressions in Eqs. (1) and (3), the Lagrangian $i\bar{c}^a \Box c^a + i\bar{c}^a g f_{abc}\varphi^b c^c = 2\mathrm{tr}(i\bar{c}\Box c + \bar{c}[g\varphi, c])$ becomes

$$\sum_{A=3,8} \bar{c}^A i\Box c^A + \sum_{\alpha=1}^{3}\left\{\bar{C}^\alpha (i\Box + g\vec{\epsilon}_\alpha\cdot\vec{\varphi})C^{-\alpha} + \bar{C}^{-\alpha}(i\Box - g\vec{\epsilon}_\alpha\cdot\vec{\varphi})C^\alpha\right\}. \tag{4}$$

Next, as in the SU(2) case [7], we integrate out $C^{\pm\alpha}$ and $\bar{C}^{\mp\alpha}$ with the momentum $\mu \le k \le \Lambda$. After the Wick rotation, we obtain the potential

$$\begin{aligned}\sum_{\alpha=1}^{3} V_1(\vec{\epsilon}_\alpha\cdot\vec{\varphi}) &= -\sum_{\alpha=1}^{3}\int_\mu^\Lambda \frac{d^4k}{(2\pi)^4}\ln\left[(-k^2)^2 + g^2(\vec{\epsilon}_\alpha\cdot\vec{\varphi})^2\right] \\ &= -\frac{1}{32\pi^2}\sum_{\alpha=1}^{3}\left[\left\{\Lambda^4 + g^2(\vec{\epsilon}_\alpha\cdot\vec{\varphi})^2\right\}\ln\left\{\Lambda^4 + g^2(\vec{\epsilon}_\alpha\cdot\vec{\varphi})^2\right\}\right. \\ &\quad \left. - \left\{\mu^4 + g^2(\vec{\epsilon}_\alpha\cdot\vec{\varphi})^2\right\}\ln\left\{\mu^4 + g^2(\vec{\epsilon}_\alpha\cdot\vec{\varphi})^2\right\}\right].\end{aligned}$$

Since we can rewrite $\varphi^a\varphi^a/(2\alpha_2)$ as

$$\frac{1}{2\alpha_2}\varphi^a\varphi^a = \frac{1}{2\alpha_2}\vec{\varphi}\cdot\vec{\varphi} = \frac{1}{3\alpha_2}\sum_{\alpha=1}^{3}(\vec{\epsilon}_\alpha\cdot\vec{\varphi})^2,$$

the one-loop effective potential of φ becomes [8]

$$V(\varphi) = \sum_{\alpha=1}^{3}\left[\frac{(\vec{\epsilon}_\alpha\cdot\vec{\varphi})^2}{3\alpha_2} + V_1(\vec{\epsilon}_\alpha\cdot\vec{\varphi})\right]. \tag{5}$$

To study minimum points of $V(\varphi)$, we consider

$$\begin{aligned}\frac{\partial V}{\partial\varphi^8} &= \frac{\varphi^8}{\alpha_2} - \frac{3}{2}g^2\varphi^8\{L(\vec{\epsilon}_2\cdot\vec{\varphi}) + L(\vec{\epsilon}_3\cdot\vec{\varphi})\} - \frac{\sqrt{3}}{2}g^2\varphi^3\{L(\vec{\epsilon}_2\cdot\vec{\varphi}) - L(\vec{\epsilon}_3\cdot\vec{\varphi})\}, \\ \frac{\partial V}{\partial\varphi^3} &= \frac{\varphi^3}{\alpha_2} - g^2\varphi^3[2L(\vec{\epsilon}_1\cdot\vec{\varphi}) + \frac{1}{2}\{L(\vec{\epsilon}_2\cdot\vec{\varphi}) + L(\vec{\epsilon}_3\cdot\vec{\varphi})\}] - \frac{\sqrt{3}}{2}g^2\varphi^8\{L(\vec{\epsilon}_2\cdot\vec{\varphi}) - L(\vec{\epsilon}_3\cdot\vec{\varphi})\},\end{aligned}$$

$$L(\vec{\epsilon}_\alpha\cdot\vec{\varphi}) = \frac{1}{32\pi^2}\ln\left\{\frac{\Lambda^4 + (g\vec{\epsilon}_\alpha\cdot\vec{\varphi})^2}{\mu^4 + (g\vec{\epsilon}_\alpha\cdot\vec{\varphi})^2}\right\}.$$

The explicit forms of $g\vec{\epsilon}_\alpha\cdot\vec{\varphi}$ ($\alpha = 1, 2, 3$) are

$$g\vec{\epsilon}_1\cdot\vec{\varphi} = g\varphi^3, \qquad g\vec{\epsilon}_2\cdot\vec{\varphi} = -\frac{g}{2}\left(\varphi^3 + \sqrt{3}\varphi^8\right), \qquad g\vec{\epsilon}_3\cdot\vec{\varphi} = \frac{g}{2}\left(-\varphi^3 + \sqrt{3}\varphi^8\right),$$

and $\varphi^8 = 0$ leads to $\vec{\epsilon}_2\cdot\vec{\varphi} = \vec{\epsilon}_3\cdot\vec{\varphi}$. So, the equation $\partial V/\partial\varphi^8 = 0$ has the solution $\varphi^8 = 0$. Now we assume that $\langle g\vec{\varphi}\rangle = (v, 0)$ is a minimum point. Since the potential $V(\varphi)$ is invariant under the interchange $\vec{\epsilon}_\alpha\cdot\vec{\varphi} \longleftrightarrow \vec{\epsilon}_\beta\cdot\vec{\varphi}$ ($\alpha \neq \beta$), and has the symmetry $\vec{\epsilon}_\alpha\cdot\vec{\varphi} \to -\vec{\epsilon}_\alpha\cdot\vec{\varphi}$, there are six

minimum points:[1]

$$\begin{array}{lll} (v,0), & \left(-\frac{v}{2},-\frac{\sqrt{3}}{2}v\right), & \left(-\frac{v}{2},\frac{\sqrt{3}}{2}v\right), \\ (-v,0), & \left(\frac{v}{2},\frac{\sqrt{3}}{2}v\right), & \left(\frac{v}{2},-\frac{\sqrt{3}}{2}v\right). \end{array} \tag{6}$$

To determine the value of v, we consider the case $(v, 0)$. The condition $\partial V/\partial\varphi^3 = 0$ with $g\varphi^3 = v \neq 0$ becomes

$$\frac{32\pi^2}{\alpha_2 g^2} = \ln\left\{\left(\frac{v^2+\Lambda^4}{v^2+\mu^4}\right)^2\left(\frac{v^2+4\Lambda^4}{v^2+4\mu^4}\right)\right\}. \tag{7}$$

If we set $v = 0$ at $\mu = \mu_0$, $\mu_0 = \Lambda\exp[-8\pi^2/3\alpha_2 g^2]$ is obtained. When the cut-off Λ is large enough, Eq. (7) gives $v \simeq 2^{1/3}\mu_0^2$ in the limit $\mu \to 0$.

In Appendix A, we show that $3\alpha_2 = \beta_0$ is the ultraviolet fixed point of α_2, where $\beta_0 = 11N/3$ with $N = 3$ is the first coefficient of the β function. Substituting this value into μ_0, we find

$$\mu_0 = \Lambda\exp\left[-\frac{8\pi^2}{\beta_0 g^2}\right] = \Lambda_{\rm QCD},$$

where $\Lambda_{\rm QCD}$ is the QCD scale parameter. Thus, we obtain the ghost condensate v that behaves as

$$v = 0 \quad (\mu \geq \Lambda_{\rm QCD}), \qquad v \neq 0 \quad (\mu < \Lambda_{\rm QCD}), \qquad v \simeq 2^{1/3}\Lambda_{\rm QCD}^2 \quad (\mu \to 0).$$

3. Gluon mass

3.1 *Tachyonic gluon mass*

In the SU(2) gauge theory, ghost loops with $v \neq 0$ produce the tachyonic gluon mass terms [6,9]. To study the SU(3) case, we choose the vacuum $(v, 0)$ in Eq. (6), and write $g\varphi^a = v\delta^{3a} + g\tilde{\varphi}^a$, where $\tilde{\varphi}^a$ is the quantum part. Neglecting $\tilde{\varphi}^a$, the Lagrangian in Eq. (4) becomes

$$\sum_{A=3,8} i\bar{c}^A\Box c^A + \sum_{\alpha=1}^{3}\left\{i\bar{C}^\alpha\left(\Box - i\epsilon_\alpha^3 v\right)C^{-\alpha} + i\bar{C}^{-\alpha}\left(\Box + i\epsilon_\alpha^3 v\right)C^\alpha\right\},$$

and it leads to the ghost propagators

$$\begin{aligned} \langle c^A\bar{c}^A\rangle &= -\frac{i}{\Box} \qquad (A = 3, 8), \\ \langle C^\alpha\bar{C}^{-\alpha}\rangle &= -\frac{i}{\Box + i\epsilon_\alpha^3 v}, \qquad \langle C^{-\alpha}\bar{C}^\alpha\rangle = -\frac{i}{\Box - i\epsilon_\alpha^3 v} \qquad (\alpha = 1, 2, 3). \end{aligned} \tag{8}$$

Using Eqs. (1) and (3), the vertex $-i\partial_\mu\bar{c}^a g f_{abc}A^{b\mu}c^c$ in $i\bar{c}^a(\partial_\mu D^\mu)^{ab}c^b$ is rewritten as

$$\begin{aligned} &\sum_{A=3,8}\Bigg[-gA^{A\mu}\sum_{\alpha=1}^{3}\epsilon_\alpha^A\left\{(\partial_\mu\bar{C}^\alpha)C^{-\alpha} - (\partial_\mu\bar{C}^{-\alpha})C^\alpha\right\} \\ &\quad + g(\partial_\mu\bar{c}^A)\sum_{\alpha=1}^{3}\epsilon_\alpha^A(W^{\alpha\mu}C^{-\alpha} - W^{-\alpha\mu}C^\alpha) - g\sum_{\alpha=1}^{3}\epsilon_\alpha^A\left\{W^{\alpha\mu}(\partial_\mu\bar{C}^{-\alpha}) - W^{-\alpha\mu}(\partial_\mu\bar{C}^\alpha)\right\}c^A\Bigg] \\ &\quad + \sum_{(\alpha,\beta,\gamma)}{\rm sgn}(\gamma)\frac{g}{\sqrt{2}}\epsilon_{\alpha\beta\gamma}(\partial_\mu\bar{C}^\alpha)C^\beta W^{\gamma\mu}, \end{aligned} \tag{9}$$

where ${\rm sgn}(\gamma)$ is the sign of γ, and $\sum_{(\alpha,\beta,\gamma)}$ implies the sum for the permutations of (1,2,3) and $(-1, -2, -3)$.

[1] These minimum points were found in Ref. [8], which also contains a three-dimensional figure of $V(\varphi)$.

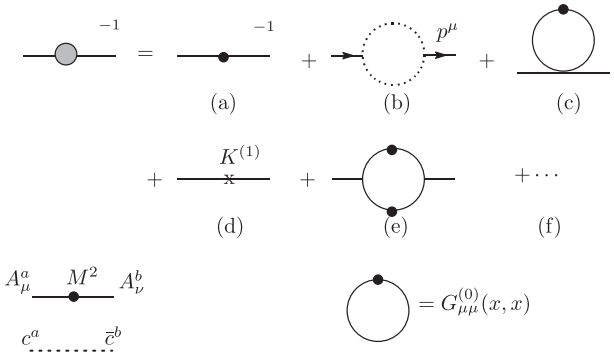

Fig. 1. The diagrams that contribute to the inverse propagator for A^a_μ; (b) gives rise to the tachyonic mass in the limit $p \to 0$, and (c) yields the condensate $G^{(0)}_{\mu\mu}(x,x)$.

Now we consider the two-point function

$$\left\langle A^a_\mu(x) A^b_\nu(y) \right\rangle = G^{ab}_{\mu\nu}(x,y) \tag{10}$$

at the one-loop level. As in the SU(2) case, using the ghost propagators in Eq. (8) and the interactions in Eq. (9), the ghost loop in Fig. 1(b) gives rise to tachyonic masses in the low-momentum limit $p \to 0$. The details are presented in Appendix B. From Eqs. (B3) and (B7), we find that the tachyonic mass terms are

$$-\frac{1}{2}\left(\frac{5}{2}m^2\right) A^{3\mu} A^3_\mu - \frac{1}{2}\left(\frac{3}{2}m^2\right) A^{8\mu} A^8_\mu - \sum_{\alpha=1}^{3}\left(\frac{5}{4}m^2\right) W^{\alpha\mu} W^{-\alpha}_\mu, \qquad m^2 = \frac{g^2 v}{64\pi}. \tag{11}$$

3.2 *Condensate* $\langle A^{a\mu} A^a_\mu \rangle$

To remove the tachyonic masses, we consider the condensate $\langle A^{a\mu} A^a_\mu \rangle$ [2,3]. Let us introduce the source terms

$$\sum_{A=3,8} K_A A^{A\mu} A^A_\mu + \sum_{\alpha=1}^{3} \mathcal{K}_\alpha W^{\alpha\mu} W^\alpha_\mu.$$

Although the sources may depend on the momentum scale, for simplicity, the constant sources

$$\begin{aligned} K_A &= K^{(0)}_A + K^{(1)}_A + \cdots, & K^{(n)}_A &= O(\hbar^n), & K^{(0)}_A &= \tfrac{1}{2} M^2_A & (A = 3, 8), \\ \mathcal{K}_\alpha &= \mathcal{K}^{(0)}_\alpha + \mathcal{K}^{(1)}_\alpha + \cdots, & \mathcal{K}^{(n)}_\alpha &= O(\hbar^n), & \mathcal{K}^{(0)}_\alpha &= \mathcal{M}^2_\alpha & (\alpha = 1, 2, 3) \end{aligned}$$

are considered. The interaction $-(g f_{abc} A^b_\mu A^c_\nu)^2/4$ in $-(F^a_{\mu\nu})^2/4$ contains the terms

$$\begin{aligned} &-\frac{g^2}{2}\sum_{\alpha=1}^{3} W^{\alpha\mu} W^{-\alpha}_\mu W^{\alpha\nu} W^{-\alpha}_\nu - \frac{g^2}{4}\sum_{\alpha\neq\beta} W^{\alpha\mu} W^{-\alpha}_\mu W^{\beta\nu} W^{-\beta}_\nu \\ &- g^2 \sum_{\alpha=1}^{3} \left(\vec{\epsilon}_\alpha \cdot \vec{A}^\mu\right)\left(\vec{\epsilon}_\alpha \cdot \vec{A}_\mu\right) W^{\alpha\nu} W^{-\alpha}_\nu. \end{aligned} \tag{12}$$

So, at $O(\hbar)$, the diagram in Fig. 1(c) gives the condensate $\langle A^{a\mu} A^a_\mu \rangle^{(0)} = g^{\mu\nu} G^{(0)aa}_{\mu\nu}(x,x)$, where $G^{(0)ab}_{\mu\nu}(x,y)$ is the free propagator with mass M_A or $\mathcal{M}_\alpha$. If the other divergent diagrams of $O(\hbar)$ are subtracted by the terms with $K^{(1)}_A$ or $\mathcal{K}^{(1)}_\alpha$, the condensate $\langle A^{a\mu} A^a_\mu \rangle^{(0)}$ is determined to remove the tachyonic masses in Eq. (11).

As an example, we consider the self-energy of W^1_μ in the limit $p \to 0$. The diagram in Fig. 1(c) with the first interaction in Eq. (12) gives $-g^2 \langle W^{1\mu} W^{-1}_\mu \rangle^{(0)}$. Similarly, from the second term in Eq. (12), we obtain $-g^2 \left[\langle W^{2\mu} W^{-2}_\mu \rangle^{(0)} + \langle W^{3\mu} W^{-3}_\mu \rangle^{(0)} \right]/2$. Since $\vec{\epsilon}_1 \cdot \vec{A}_\mu = A^3_\mu$, the third term

in Eq. (12) gives $-g^2\langle A^{3\mu}A^3_\mu\rangle^{(0)}$. So, Fig. 1(c) for W^1_μ leads to $-g^2\left\{\mathcal{G}^1+\frac{1}{2}\left(\mathcal{G}^2+\mathcal{G}^3\right)+G^3\right\}$, where $\mathcal{G}^\alpha=\langle W^{\alpha\mu}W^{-\alpha}_\mu\rangle^{(0)}$ ($\alpha=1,2,3$) and $G^A=\langle A^{A\mu}A^A_\mu\rangle^{(0)}$ ($A=3,8$). The condition that these condensates remove the tachyonic mass of W^1_μ becomes

$$-\frac{5}{4}m^2-g^2\left\{\mathcal{G}^1+\frac{1}{2}\left(\mathcal{G}^2+\mathcal{G}^3\right)+G^3\right\}=0.$$

In the same way, we find the conditions

$$-\frac{5}{4}m^2-g^2\left\{\mathcal{G}^2+\frac{1}{2}\left(\mathcal{G}^3+\mathcal{G}^1\right)+\frac{1}{4}\left(G^3+3G^8\right)\right\}=0, \tag{13}$$

$$-\frac{5}{4}m^2-g^2\left\{\mathcal{G}^3+\frac{1}{2}\left(\mathcal{G}^1+\mathcal{G}^2\right)+\frac{1}{4}\left(G^3+3G^8\right)\right\}=0,$$

$$-\frac{5}{4}m^2-g^2\left\{\mathcal{G}^1+\frac{1}{4}\left(\mathcal{G}^2+\mathcal{G}^3\right)\right\}=0, \tag{14}$$

$$-\frac{3}{4}m^2-\frac{3g^2}{4}\left(\mathcal{G}^2+\mathcal{G}^3\right)=0, \tag{15}$$

for W^2_μ, W^3_μ, A^3_μ, and A^8_μ, respectively.

The solutions of these five equations are

$$\mathcal{G}^1=-\frac{m^2}{g^2},\qquad \mathcal{G}^2=\mathcal{G}^3=-\frac{m^2}{2g^2},\qquad G^3=\frac{m^2}{4g^2},\qquad G^8=-\frac{m^2}{12g^2}. \tag{16}$$

We note that, although the diagonal component $\langle A^{3\mu}A^3_\mu\rangle^{(0)}$ vanishes in the SU(2) case [2,3], the diagonal components $\langle A^{A\mu}A^A_\mu\rangle^{(0)}$ ($A=3,8$) do not vanish in SU(3).

3.3 *Inclusion of classical solutions*

To incorporate $U(1)_3$ and $U(1)_8$ classical solutions into the above scheme, we divide A^A_μ into the classical part b^A_μ and the quantum fluctuation a^A_μ as

$$A^A_\mu=b^A_\mu+a^A_\mu\qquad(A=3,8),$$

and divide the gauge transformation $\delta A_\mu=D_\mu(A)\varepsilon$ as

$$\delta a_\mu=D_\mu(a,W)\varepsilon,\qquad(\delta b_\mu)^a=gf_{abc}b^b\varepsilon^c,\qquad\delta W_\mu=D_\mu(a,W)\varepsilon, \tag{17}$$

where $D_\mu(A)^{ab}=\partial_\mu\delta^{ab}+gf_{acb}A^c_\mu$, and $D_\mu(a,W)$ is obtained by removing b_μ from $D_\mu(A)$, i.e. $D_\mu(a,W)=D_\mu(A)|_{b_\mu=0}$. Using the gauge-fixing function $G(a,W)=\partial_\mu A^\mu|_{b_\nu=0}+\varphi-w$, the transformation in Eq. (17) gives the ghost Lagrangian

$$i\bar{c}^a\left[\left(\partial_\mu D^\mu(A)\right)^{ac}+gf_{abc}\varphi^b\right]c^c\big|_{b_\mu=0}=i\bar{c}^a\left[\left(\partial_\mu D^\mu(a,W)\right)^{ac}+gf_{abc}\varphi^b\right]c^c.$$

So, after the ghost condensation, the tachyonic mass terms are obtained by replacing A^a_μ with a^A_μ and W^α_μ as[2]

$$-\frac{1}{2}\left(\frac{5}{2}m^2\right)a^{3\mu}a^3_\mu-\frac{1}{2}\left(\frac{3}{2}m^2\right)a^{8\mu}a^8_\mu-\sum_{\alpha=1}^{3}\left(\frac{5}{4}m^2\right)W^{\alpha\mu}W^{-\alpha}_\mu. \tag{18}$$

[2]We can use the background covariant gauge. In this case, as the ghost Lagrangian is $i\bar{c}^a\left[\left(D(b)_\mu D^\mu(A)\right)^{ac}+gf_{abc}\varphi^b\right]c^c$, $\bar{c}$ and c couple with b_μ. However, this ghost Lagrangian has the $U(1)_3\times U(1)_8$ symmetry $\delta_\varepsilon b_\mu=-\partial_\mu\vec{\varepsilon}\cdot\vec{H}/g$, $\delta_\varepsilon a_\mu=0$, and $\delta_\varepsilon W^{\pm\alpha}_\mu=\mp i\vec{\varepsilon}\cdot\vec{\epsilon}_\alpha W^{\pm\alpha}_\mu$. Therefore, as in the SU(2) case [2], this symmetry prevents b^A_μ from getting tachyonic mass terms, and Eq. (18) is obtained.

The above tachyonic mass terms are removed by the condensates $\mathcal{G}^\alpha = \langle W^{\alpha\mu} W_\mu^{-\alpha}\rangle^{(0)}$ ($\alpha = 1$, 2, 3) and $G^A = \langle a^{A\mu} a_\mu^A\rangle^{(0)}$ ($A = 3$, 8) in Eq. (16). When $\mathcal{G}^\alpha \neq 0$, the interaction

$$-g^2 \sum_{\alpha=1}^{3} \left(\vec{\epsilon}_\alpha \cdot (\vec{a}+\vec{b})^\mu\right)\left(\vec{\epsilon}_\alpha \cdot (\vec{a}+\vec{b})_\mu\right) W^{\alpha\nu} W_\nu^{-\alpha}$$

in Eq. (12) leads to the mass terms

$$-g^2 \sum_{\alpha=1}^{3} (\vec{\epsilon}_\alpha \cdot \vec{b}^\mu)(\vec{\epsilon}_\alpha \cdot \vec{b}_\mu)\mathcal{G}^\alpha = -g^2 \left\{\mathcal{G}^1 + \frac{1}{4}\left(\mathcal{G}^2 + \mathcal{G}^3\right)\right\} b^{3\mu} b_\mu^3 - \frac{3g^2}{4}\left(\mathcal{G}^2 + \mathcal{G}^3\right) b^{8\mu} b_\mu^8.$$

Since the classical part b_μ^A has no tachyonic mass, Eqs. (14) and (15) imply that these mass terms become

$$\sum_{A=3,8} \frac{m_A^2}{2} b^{A\mu} b_\mu^A, \qquad m_3^2 = \frac{5m^2}{2}, \qquad m_8^2 = \frac{3m^2}{2}. \tag{19}$$

Thus, after integrating out c and $\bar{c}$, we obtain the low-energy effective Lagrangian

$$\begin{aligned}
\mathcal{L}_{\text{e}_} &= \mathcal{L}_{\text{cl}} + \sum_{A=3,8} \left\{-\frac{1}{4}(\partial \wedge a^A)^{\mu\nu}(\partial \wedge a^A)_{\mu\nu} + \frac{M_A^2}{2} a^{A\mu} a_\mu^A\right\} \\
&\quad + \sum_{\alpha=1}^{3} \left\{-\frac{1}{4}(\partial \wedge W^\alpha)^{\mu\nu}(\partial \wedge W^\alpha)_{\mu\nu} + \mathcal{M}_\alpha^2 W^{\alpha\mu} W_\mu^\alpha\right\} + \cdots, \\
\mathcal{L}_{\text{cl}} &= \sum_{A=3,8} \left\{-\frac{1}{4}(\partial \wedge b^A)^{\mu\nu}(\partial \wedge b^A)_{\mu\nu} + \frac{m_A^2}{2} b^{A\mu} b_\mu^A\right\},
\end{aligned} \tag{20}$$

where $(\partial \wedge A^a)_{\mu\nu} = \partial_\mu A_\nu^a - \partial_\nu A_\mu^a$.

We ignored the momentum dependence of the sources K_A and $\mathcal{K}_\alpha$, and applied the $\hbar$ expansion. Because it is difficult to modify this treatment, we use $\mathcal{L}_{\text{cl}}$ as the first approximation of the low-energy Lagrangian.

4. Classical fields and static potential

4.1 *The classical electric potential $\tilde{B}_\mu^A$ and its dual potential $\mathcal{B}_\mu^A$*

It is expected that the Abelian component of the gauge field dominates in confinement [10]. Based on Refs. [3,11], we choose the dual electric potential $\mathcal{B}_\mu^A$ as the classical field b_μ^A ($A = 3, 8$). This describes the electric monopole solution [3]. The color electric current j_μ^A is incorporated by the replacement

$$(\partial \wedge \mathcal{B}^A)^{\mu\nu} \to {}^d F^{A\mu\nu} = (\partial \wedge \mathcal{B}^A)^{\mu\nu} + \epsilon^{\mu\nu\alpha\beta}(n\cdot\partial)^{-1} n_\alpha j_\beta^A,$$

where the space-like vector n^μ [4] is chosen as $n^\mu = (0, \boldsymbol{n})$ with $|\boldsymbol{n}| = 1$, and $n \cdot \partial = n^\mu \partial_\mu$. We note that this is Zwanziger's dual field strength $F^d = (\partial \wedge B) + (n\cdot\partial)^{-1}(n \wedge j_e)^d$ in Ref. [4]. Then, the Lagrangian in Eq. (20) becomes

$$\mathcal{L}_{\text{cl}} = \sum_{A=3,8} \left[-\frac{1}{4}\left\{(\partial \wedge \mathcal{B}^A)^{\mu\nu} + \epsilon^{\mu\nu\alpha\beta}(n\cdot\partial)^{-1} n_\alpha j_\beta^A\right\}^2 + \frac{m_A^2}{2}\left(\mathcal{B}_\mu^A\right)^2\right]. \tag{21}$$

The equation of motion for $\mathcal{B}_\mu^A$ is

$$(D_{m_A}^{-1})^{\mu\nu} \mathcal{B}_\nu^A = -\epsilon^{\mu\rho\alpha\beta}(n\cdot\partial)^{-1} n_\rho \partial_\alpha j_\beta^A, \qquad (D_{m_A}^{-1})^{\mu\nu} = (\Box + m_A^2) g^{\mu\nu} - \partial^\mu \partial^\nu, \tag{22}$$

and $\mathcal{B}_\mu^A$ is solved as

$$\mathcal{B}_\mu^A = -(D_{m_A})_{\mu\nu} \epsilon^{\nu\rho\alpha\beta}(n\cdot\partial)^{-1} n_\rho \partial_\alpha j_\beta^A, \qquad (D_{m_A})_{\mu\nu} = \frac{g_{\mu\nu} - \partial_\mu\partial_\nu/\Box}{\Box + m_A^2} + \frac{\partial_\mu \partial_\nu}{m_A^2 \Box}. \tag{23}$$

If we use Eq. (23), Eq. (21) becomes

$$\mathcal{L}_{jj} = \sum_{A=3,8} \left[-\frac{1}{2} j_\mu^A \frac{1}{\Box + m_A^2} j^{A\mu} - \frac{1}{2} j_\mu^A \frac{m_A^2}{\Box + m_A^2} \frac{n\cdot n}{(n\cdot\partial)^2} \left(g^{\mu\nu} - \frac{n^\mu n^\nu}{n\cdot n} \right) j_\nu^A \right]. \tag{24}$$

Although we used the dual electric potential $\mathcal{B}_\mu^A$ above, we can use the electric potential $\tilde{B}_\mu^A$. The relation between $\tilde{B}_\mu^A$ and $\mathcal{B}_\mu^A$ is [3]

$$\begin{aligned} -\epsilon^{\mu\nu\alpha\beta}\partial_\alpha \mathcal{B}_\beta^A &= (\partial \wedge \tilde{B}^A)^{\mu\nu} + \Lambda_e^{A\mu\nu}, \\ \Lambda_e^{A\mu\nu} &= -\frac{n^\mu}{n\cdot\partial}\partial_\sigma (\partial \wedge \tilde{B}^A)^{\sigma\nu} + \frac{n^\nu}{n\cdot\partial}\partial_\sigma (\partial \wedge \tilde{B}^A)^{\sigma\mu}. \end{aligned} \tag{25}$$

The dual potential $\mathcal{B}_\mu^A$ has the electric correspondent of the Dirac string, which we call the electric string. The term $\Lambda_e^{A\mu\nu}$ represents this string.[3] The field $\tilde{B}_\mu^A$ satisfies the equation of motion

$$(D_{m_A}^{-1})_{\mu\nu}\tilde{B}^{A\nu} - j_\mu^A = 0,$$

and the Lagrangian that is equivalent to Eq. (21) is [3]

$$\mathcal{L}_{\rm ecl} = \sum_{A=3,8} \left\{ -\frac{1}{4}(\partial \wedge \tilde{B}^A)^2 + \frac{m_A^2}{2}\tilde{B}_\mu^A \tilde{B}^{A\mu} - \tilde{B}_\mu^A j^{A\mu} - \frac{m_A^2}{2}\tilde{B}^{A\mu}\frac{n\cdot n}{(n\cdot\partial)^2}\left(g_{\mu\nu} - \frac{n_\mu n_\nu}{n\cdot n} \right) j^{A\nu} \right\}.$$

The last term comes from the electric string. Substituting $\tilde{B}^{A\mu} = (D_{m_A})^{\mu\nu} j_\nu^A$ into $\mathcal{L}_{\rm ecl}$, we can obtain $\mathcal{L}_{jj}$ in Eq. (24).

4.2 *Potential between static charges*

We consider the static charges Q_a^A at $\boldsymbol{a}$ and Q_b^A at $\boldsymbol{b}$. Substituting the static current

$$j_\mu^A(x) = g_{\mu 0}\left\{ Q_a^A \delta(\boldsymbol{x} - \boldsymbol{a}) + Q_b^A \delta(\boldsymbol{x} - \boldsymbol{b}) \right\} \tag{26}$$

into $\mathcal{L}_{jj}$, we get the potential

$$V(\boldsymbol{r}) = \sum_{A=3,8} \left\{ V_Y^A(r) + V_L^A(\boldsymbol{r}) \right\},$$

$$V_Y^A(r) = \int \frac{d^3q}{(2\pi)^3} \left(\frac{(Q_a^A)^2 + (Q_b^A)^2}{2} + Q_a^A Q_b^A e^{i\boldsymbol{q}\cdot\boldsymbol{r}} \right) \frac{1}{q^2 + m_A^2}, \tag{27}$$

$$V_L^A(\boldsymbol{r}) = \int \frac{d^3q}{(2\pi)^3} \left(\frac{(Q_a^A)^2 + (Q_b^A)^2}{2} + Q_a^A Q_b^A e^{i\boldsymbol{q}\cdot\boldsymbol{r}} \right) \frac{m_A^2}{(q^2 + m_A^2)q_n^2}, \tag{28}$$

where $\boldsymbol{r} = \boldsymbol{a} - \boldsymbol{b}$, $q = |\boldsymbol{q}|$, and $q_n = \boldsymbol{q}\cdot\boldsymbol{n}$. The first (second) term in $\mathcal{L}_{jj}$ leads to V_Y^A (V_L^A). Historically, these potentials were obtained by using the dual Ginzburg–Landau model [12–15]. These potentials are calculated in Appendix D. Assuming that m_A disappears above the scale $\Lambda_{\rm c}$, Eq. (27) gives [16]

$$\begin{aligned} V_Y^A(r) &= Q_a^A Q_b^A \left(\frac{1}{4\pi r} - \frac{m_A^2}{2\pi^2}\int_0^{\Lambda_{\rm c}} dq \frac{\sin qr}{qr}\frac{1}{q^2 + m_A^2} \right) = -\frac{Q_a^A Q_b^A}{g^2}\left(-\frac{\alpha^A(r)}{r} \right), \\ \alpha^A(r) &= \frac{g^2}{4\pi} - \frac{g^2 m_A^2 r}{2\pi^2}\int_0^{\Lambda_{\rm c}} dq \frac{\sin qr}{qr}\frac{1}{q^2 + m_A^2}. \end{aligned} \tag{29}$$

The first term in $V_Y^A(r)$ is the usual Coulomb potential, which is the main term for small r.

[3] In Appendix C, as an example, we present the massless fields $\tilde{B}_\mu^A$ and $\mathcal{B}_\mu^A$ for a point charge, and show that $\Lambda_e^{A\mu\nu}$ describes the electric string. The relation in Eq. (25) is also used to consider the color electric flux in Sect. 6.

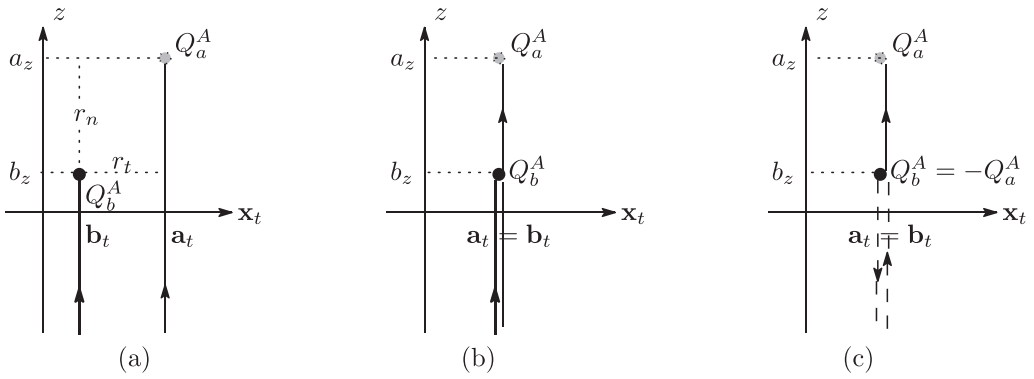

Fig. 2. The relation between the conditions in Eq. (34) and the length of the electric string. Case (a), with $r_t \neq 0$, and case (b), with ($r_t = 0$, $Q_a^A + Q_b^A \neq 0$), have the string with infinite length. The length of the string in case (c), which satisfies Eq. (34), is finite.

Under the same assumption that $m_A = 0$ above Λ_c, Eq. (28) gives

$$V_L^A(\boldsymbol{r}) = V_{\rm IR}^A(r_t) - \frac{Q_a^A Q_b^A m_A^2}{4\pi} K_0(m_A r_t, \Lambda_c) r_n + \cdots, \tag{30}$$

$$V_{\rm IR}^A(r_t) = \frac{m_A^2}{2\pi^2\varepsilon}\left\{\frac{\left(Q_a^A\right)^2 + \left(Q_b^A\right)^2}{2m_A}\tan^{-1}\frac{\Lambda_c}{m_A} + Q_a^A Q_b^A H(m_A, \Lambda_c, r_t)\right\}, \tag{31}$$

where the functions $K_0(m_A r_t, \Lambda_c)$ and $H(m_A, \Lambda_c, r_t)$ are defined in Eq. (D10). We have chosen $\boldsymbol{n}$ as $r_n = \boldsymbol{r}\cdot\boldsymbol{n} \geq 0$, and $\boldsymbol{r} = (r_n, \boldsymbol{r}_t)$. The vector $\boldsymbol{r}_t$ satisfies $\boldsymbol{r}_t \perp \boldsymbol{n}$, and $r_t = |\boldsymbol{r}_t|$. The term $V_{\rm IR}^A$ has infrared divergence $1/\varepsilon$, where the infrared cut-off ε satisfies $0 < \varepsilon \ll 1$. To remove this divergence, since the direction $\boldsymbol{n}$ of the electric string is arbitrary, we choose $\boldsymbol{r} \parallel \boldsymbol{n}$ [3,15,16]. In this case, as $(r_n, r_t) = (r, 0)$, Eq. (30) becomes

$$V_L^A(r) = V_{\rm IR}^A - \frac{Q_a^A Q_b^A}{g^2}\sigma^A r + \cdots, \qquad \sigma^A = \frac{g^2 m_A^2}{8\pi}\ln\left(\frac{\Lambda_c^2 + m_A^2}{m_A^2}\right), \tag{32}$$

$$V_{\rm IR}^A = \frac{m_A}{4\pi^2\varepsilon}\left(Q_a^A + Q_b^A\right)^2 \tan^{-1}\frac{\Lambda_c}{m_A}, \tag{33}$$

where $K_0(0, \Lambda_c)$ and $H(m_A, \Lambda_c, 0)$ are presented in Eq. (D11). Equation (33) shows that $V_{\rm IR}^A$ vanishes if $Q_a^A + Q_b^A = 0$. Therefore, the conditions to remove the infrared divergence are

$$r_t = 0, \qquad Q_a^A + Q_b^A = 0. \tag{34}$$

When Eq. (34) holds, the leading term of Eq. (32) is the linear potential $-(Q_a^A Q_b^A/g^2)\sigma^A r$, which is the main term for large r.

We note the infrared divergence implies the existence of the electric string with infinite length and mass m_A. The relation between the conditions in Eq. (34) and the length of the electric string are depicted in Fig. 2.

In the SU(2) case, comparing the $q\bar{q}$ potential with $V_Y(r)$ and $V_L(r)$, we tried to determine the values of parameters, and reproduce the Coulomb plus linear type potential [16]. However, in the SU(3) case, there are many parameters like M_A ($A = 3, 8$) and $\mathcal{M}_\alpha$ ($\alpha = 1, 2, 3$). In addition, since $m_3 \neq m_8$, we are not sure whether a single cut-off Λ_c is usable or not. So we do not try to determine the parameters in this paper. Instead, below we study the consequences derived from the Lagrangian in Eq. (21) and the potentials in Eqs. (29) and (32).

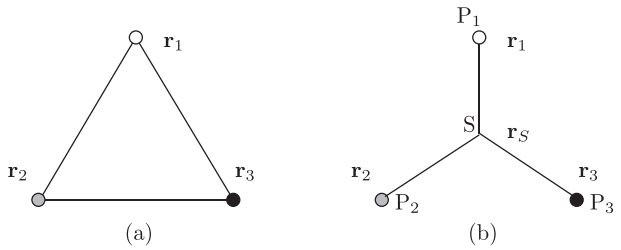

Fig. 3. The color flux between the charges. (a) is the Δ-type baryon and (b) is the Y-type baryon.

5. Mesonic and baryonic potentials

5.1 *Notation*

Corresponding to the three types of color charge, red, blue, and green, we use C_1, C_2, and C_3, respectively. The quark field is $\Psi = {}^t(\psi_{C_1}\ \psi_{C_2}\ \psi_{C_3})$, and the current $j^A_\mu = g\bar{\Psi}\gamma_\mu H^A \Psi$ $(A = 3, 8)$ is written as

$$j^A_\mu = \sum_{i=1}^{3} g w^A_i \bar{\psi}_{C_i}\gamma_\mu \psi_{C_i},$$

where the weight vectors are

$$\vec{w}_1 = \left(\frac{1}{2}, \frac{1}{2\sqrt{3}}\right), \qquad \vec{w}_2 = \left(\frac{-1}{2}, \frac{1}{2\sqrt{3}}\right), \qquad \vec{w}_3 = \left(0, -\frac{1}{\sqrt{3}}\right). \tag{35}$$

When we use the static potentials in Eqs. (29)–(33), the static charges are given by

$$Q^A_{C_j} = g w^A_j = -\bar{Q}^A_{C_j} \qquad (A = 3, 8;\ \ j = 1, 2, 3). \tag{36}$$

5.2 *Mesonic potential*

If a static quark (an antiquark) exists at $\boldsymbol{a}$ ($\boldsymbol{b}$), a meson is expressed by

$$\frac{1}{\sqrt{3}} \sum_{i=1}^{3} |q_{C_i}(\boldsymbol{a})\bar{q}_{C_i}(\boldsymbol{b})\rangle$$

We set $Q^A_a = Q^A_{C_i}$, $Q^A_b = \bar{Q}^A_{C_i} = -Q^A_{C_i}$, and $\boldsymbol{r} = (\boldsymbol{a} - \boldsymbol{b}) \parallel \boldsymbol{n}$. Then the two conditions in Eq. (34) are satisfied, and V^A_{IR} vanishes. Using the relation

$$\frac{1}{3}\sum_{i=1}^{3} \frac{-Q^A_{C_i}\bar{Q}^A_{C_i}}{g^2} = \frac{1}{3}\sum_{i=1}^{3}(w^A_i)^2 = \frac{1}{6} \qquad (A = 3, 8),$$

Eqs. (29) and (32) give the mesonic potential

$$V_{q\bar{q}}(r) = \frac{1}{6}\sum_{A=3,8}\left\{-\frac{\alpha^A(r)}{r} + \sigma^A r + \cdots\right\} = -\frac{\alpha_{q\bar{q}}(r)}{r} + \sigma_{q\bar{q}} r + \cdots, \tag{37}$$

where $\alpha_{q\bar{q}}(r) = \sum_{A=3,8}\alpha^A(r)/6$ and $\sigma_{q\bar{q}} = \sum_{A=3,8}\sigma^A/6$.

5.3 *Δ-type 3q potential*

Let us study the potential for the configuration in Fig. 3(a), which is called the Δ-ansatz [17]. To apply Eqs. (29) and (32), we replace r with $r_{kl} = |\boldsymbol{r}_{kl}| = |\boldsymbol{r}_k - \boldsymbol{r}_l|$ $(k \neq l)$ and $\boldsymbol{n}$ with $\boldsymbol{n}_{kl}$, which satisfies $\boldsymbol{n}_{kl} \parallel \boldsymbol{r}_{kl}$. When static quarks are placed at $\boldsymbol{r}_k$ $(k = 1, 2, 3)$, a baryonic state is

$$\frac{1}{\sqrt{6}}\sum_{ijk}\varepsilon_{ijk}|q_{C_i}(\boldsymbol{r}_1)q_{C_j}(\boldsymbol{r}_2)q_{C_k}(\boldsymbol{r}_3)\rangle.$$

If we set $Q_a^A = Q_{C_i}^A$ and $Q_b^A = Q_{C_j}^A$ with $i \neq j$, and use the relation

$$\frac{1}{6}\sum_{i\neq j}\frac{-Q_{C_i}^A Q_{C_j}^A}{g^2} = -\frac{1}{6}\sum_{i\neq j} w_i^A w_j^A = \frac{1}{12} \qquad (A = 3, 8),$$

Eqs. (29) and (32) give

$$V_{3q}^{\Delta}(\boldsymbol{r}_1, \boldsymbol{r}_2, \boldsymbol{r}_3) = \sum_{A=3,8} V_{\mathrm{IR}}^A + \frac{1}{12}\sum_{k>l}\sum_{A=3,8}\left\{-\frac{\alpha^A(r_{kl})}{r_{kl}} + \sigma^A r_{kl} + \cdots\right\}. \tag{38}$$

We make two comments. First, from Eqs. (37) and (38), we obtain the relation [19]

$$V_{3q}^{\Delta}(\boldsymbol{r}_1, \boldsymbol{r}_2, \boldsymbol{r}_3) - \sum_{A=3,8} V_{\mathrm{IR}}^A = \frac{1}{2}\sum_{k>l} V_{q\bar{q}}(r_{kl}). \tag{39}$$

Second, by the choice $\boldsymbol{n}_{kl} \parallel \boldsymbol{r}_{kl}$, the first condition $(r_{kl})_t = 0$ is satisfied. However, except for $Q_{C_1}^3 + Q_{C_2}^3 = 0$, the second condition $Q_{C_i}^A + Q_{C_j}^A = 0$ $(i \neq j)$ does not hold. So, using

$$\frac{1}{6}\sum_{i\neq j}\frac{\left(Q_{C_i}^A + Q_{C_j}^A\right)^2}{g^2} = \frac{1}{6}\sum_{i\neq j}\left(w_i^A + w_j^A\right)^2 = \frac{1}{6} \qquad (A = 3, 8),$$

we find the infrared divergent term,

$$\sum_{A=3,8} V_{\mathrm{IR}}^A = \sum_{A=3,8}\frac{m_A}{24\pi^2\varepsilon}\tan^{-1}\frac{\Lambda_{\mathrm{c}}}{m_A}, \tag{40}$$

remains. In the Δ-ansatz, there are electric strings with infinite length. When $m_A \neq 0$, they give rise to the infrared divergence.

5.4 *Y-type 3q potential*

For large r_{kl}, the potential $V_L^A(r_{kl})$ in $V_{3q}^{\Delta}(\boldsymbol{r}_1, \boldsymbol{r}_2, \boldsymbol{r}_3)$ has the infrared divergence. On the other hand, based on the strong coupling argument, the Y-shaped baryon depicted in Fig. 3(b) was proposed [18]. The point S at $\boldsymbol{r}_S$, where the sum of the length $L_Y = \sum_{k=1}^3 r_{kS} = \sum_{k=1}^3 |\boldsymbol{r}_k - \boldsymbol{r}_S|$ becomes a minimum, is the Steiner point. The color electric flux lines emanating from the three quarks meet and disappear there. Since the state at this point is a color singlet, corresponding to the state $|q_{C_1}(\boldsymbol{r}_1)q_{C_2}(\boldsymbol{r}_2)q_{C_3}(\boldsymbol{r}_3)\rangle$, the state at $\boldsymbol{r}_S$ is $|\bar{q}_{C_1}(\boldsymbol{r}_S)\bar{q}_{C_2}(\boldsymbol{r}_S)\bar{q}_{C_3}(\boldsymbol{r}_S)\rangle$. So, when r_{kS} is large, the potential is the sum of the three $q\bar{q}$ potentials for large r. Thus, we obtain

$$V_{3qL}^{Y}(\boldsymbol{r}_1, \boldsymbol{r}_2, \boldsymbol{r}_3) = \sum_{k=1}^{3} V_{q\bar{q}L}(r_{kS}) = \frac{1}{6}\sum_{k=1}^{3}\sum_{A=3,8}(\sigma^A r_{kS} + \cdots) = \sigma_Y L_Y + \cdots, \tag{41}$$

where $\sigma_Y = \sum_{A=3,8}\sigma^A/6$.

We note that when r_{kl} is large, Eq. (38) gives

$$V_{3qL}^{\Delta}(\boldsymbol{r}_1, \boldsymbol{r}_2, \boldsymbol{r}_3) - \sum_{A=3,8} V_{\mathrm{IR}}^A = \sigma_\Delta L_\Delta + \cdots, \tag{42}$$

where $L_\Delta = \sum_{k>l} r_{kl}$ and $\sigma_\Delta = \sum_{A=3,8}\sigma^A/12$. From Eqs. (37), (41), and (42), the relations $\sigma_\Delta = \sigma_{q\bar{q}}/2$, $\sigma_Y = \sigma_{q\bar{q}}$, and

$$V_{3qL}^{\Delta}(\boldsymbol{r}_1, \boldsymbol{r}_2, \boldsymbol{r}_3) - \sum_{A=3,8} V_{\mathrm{IR}}^A = V_{3qL}^{Y}(\boldsymbol{r}_1, \boldsymbol{r}_2, \boldsymbol{r}_3) - \sigma_{q\bar{q}}\left(L_Y - \frac{1}{2}L_\Delta\right) \tag{43}$$

are obtained at this level [19]. As $L_Y > L_\Delta/2$, the inequality $V_{3qL}^{Y} > V_{3qL}^{\Delta} - \sum_{A=3,8} V_{\mathrm{IR}}^A$ holds. However, differently from V_{3qL}^{Δ}, V_{3qL}^{Y} is free from the infrared divergence.

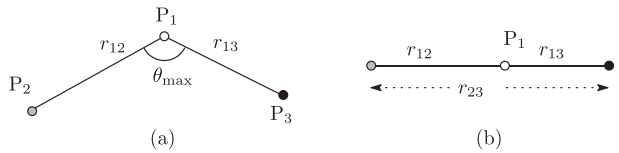

Fig. 4. The cases where the maximum inner angle $\theta_{\max}$ satisfies $120^\circ \le \theta_{\max} \le 180^\circ$.

5.5 *Comparison with lattice results*

In the present model, the classical Abelian potentials $\mathcal{B}^A_\mu$ ($A = 3, 8$) lead to the linear potential. The Y-type potential is preferable to the Δ-type potential, because the former has no infrared divergence. The string tension of the Y-type potential satisfies $\sigma_Y = \sigma_{q\bar{q}}$.

In the lattice simulation, the $3q$ baryon has been studied, and the Y-type potential is obtained [20–22]. In Ref. [21], using the maximal Abelian gauge, it was shown that the three-quark string tension σ_{3q} satisfies $\sigma_{3q} \simeq \sigma_{q\bar{q}}$. In addition, the string tensions $\sigma^{\rm Abel}_{3q}$ and $\sigma^{\rm Abel}_{q\bar{q}}$, which are obtained from the Abelian part, satisfy $\sigma_{3q} \simeq \sigma^{\rm Abel}_{3q}$ and $\sigma_{q\bar{q}} \simeq \sigma^{\rm Abel}_{q\bar{q}}$ within a few percent deviation. These results show that the potential is Y-type, and the Abelian dominance is realized.

In Ref. [22], using the Polyakov loop correlation function, the cases with $60^\circ \le \theta_{\max} < 120^\circ$ and $120^\circ \le \theta_{\max} \le 180^\circ$ were simulated, where $\theta_{\max}$ represents the maximum inner angle of a triangle. In the latter case, the Steiner point S is the point P_1 in Fig. 4. As $r_{1S} = 0$ in this case, the length L_Y is reduced to $L_Y = r_{12} + r_{13} = L_\Delta - r_{23}$. When $120^\circ \le \theta_{\max} < 180^\circ$, they found that the long-range potential satisfies $V_{3qL} \simeq \sigma_{q\bar{q}} L_Y$, and $\sigma_{3q} \simeq \sigma_{q\bar{q}}$ holds. On the other hand, when $\theta_{\max} = 180^\circ$, they obtained the Δ-type relation $V_{3q} = \frac{1}{2}\sum_{k>l} V_{q\bar{q}}(r_{kl})$.

In our approach, when $120^\circ \le \theta_{\max} \le 180^\circ$, the Y-type potential is calculable by setting $r_{1S} = 0$, $r_{2S} = r_{12}$, and $r_{3S} = r_{13}$. The result is

$$V^Y_{3qL} = \sigma_Y L_Y = \sigma_{q\bar{q}} L_Y, \qquad L_Y = r_{12} + r_{13}. \tag{44}$$

When $\theta_{\max} = 180^\circ$, Fig. 4(b) shows that $r_{23} = r_{12} + r_{13}$ and $L_Y = L_\Delta/2$. As $\sigma_\Delta = \frac{1}{2}\sigma_Y$, we find that Eq. (44) becomes

$$\sigma_\Delta L_\Delta = \frac{1}{2}\sigma_{q\bar{q}} L_\Delta, \qquad L_\Delta == r_{12} + r_{13} + r_{23} = 2L_Y. \tag{45}$$

Namely, if $\theta_{\max} = 180^\circ$, the Y-type relation in Eq. (44) coincides with the Δ-type relation in Eq. (45), which is expected from Eq. (43). Therefore, we can say that the long-range potential is Y-type for $\theta_{\max} \le 180^\circ$.

6. Color electric flux

6.1 *Extended Maxwell equations*

In Sect. 4 we introduced the electric potential $\tilde{B}^A_\mu$ and its dual potential $\mathcal{B}^A_\mu$ that are related by Eq. (25). We also used Zwanziger's dual field strength ${}^dF^{A\mu\nu}$ [4] in the presence of the current j^A_μ. In this subsection, we study Maxwell's equations.

Using $\mathcal{B}^A_\mu$ and $\tilde{B}^A_\mu$, the dual field strength is expressed by

$${}^dF^{A\mu\nu} = (\partial \wedge \mathcal{B}^A)^{\mu\nu} + \frac{1}{n\cdot\partial}\epsilon^{\mu\nu\alpha\beta} n_\alpha j^A_\beta = \epsilon^{\mu\nu\alpha\beta}\partial_\alpha \tilde{B}^A_\beta - \frac{1}{n\cdot\partial}\epsilon^{\mu\nu\alpha\beta} n_\alpha \left\{\partial\cdot(\partial\wedge\tilde{B}^A) - j^A\right\}_\beta,$$

and the field strength is

$$F^{A\mu\nu} = -\epsilon^{\mu\nu\alpha\beta}\partial_\alpha \mathcal{B}^A_\beta + \frac{1}{n\cdot\partial}(n\wedge j^A)^{\mu\nu} = (\partial\wedge\tilde{B}^A)^{\mu\nu} - \frac{1}{n\cdot\partial}\left[n\wedge\left\{\partial\cdot(\partial\wedge\tilde{B}^A) - j^A\right\}\right]^{\mu\nu}.$$

The electric field $E^{Ai}(j) = F^{Ai0}$ and the magnetic field $H^{Ai}(j) = {}^dF^{Ai0}$ are

$$E^{Ai}(j) = -\epsilon^{ijk}\partial_j \mathcal{B}^{Ak} + \frac{n^i}{n\cdot\partial} j^{A0}$$
$$= -\partial_i \tilde{B}^{A0} - \partial_0 \tilde{B}^{Ai} - \frac{n^i}{n\cdot\partial}\left\{\partial\cdot(\partial\wedge\tilde{B}^A) - j^A\right\}^0, \tag{46}$$

$$H^{Ai}(j) = -\partial_i \mathcal{B}^{A0} - \partial_0 \mathcal{B}^{Ai} - \epsilon^{ijk}\frac{n^j}{n\cdot\partial} j^{Ak}$$
$$= \epsilon^{ijk}\partial_j \tilde{B}^{Ak} + \epsilon^{ijk}\frac{n^j}{n\cdot\partial}\left\{\partial\cdot(\partial\wedge\tilde{B}^A) - j^A\right\}^k, \tag{47}$$

where $n^0 = 0$ has been used. From these expressions, it is easy to show the two Maxwell equations

$$\nabla\cdot\boldsymbol{E}^A(j) = j^{A0}, \qquad \nabla\times\boldsymbol{H}^A(j) - \partial_0\boldsymbol{E}^A(j) = \boldsymbol{j}^A. \tag{48}$$

Next, we consider the remaining two Maxwell equations. Using $\mathcal{B}^{A\mu}$, Eq. (47) gives

$$\partial_i H^{Ai}(j) = \partial_i\left(-\partial_i\mathcal{B}^{A0} - \partial_0\mathcal{B}^{Ai} - \epsilon^{ijk}\frac{n^j}{n\cdot\partial}j^{Ak}\right) = \partial\cdot(\partial\wedge\mathcal{B}^A)^0 - \mathcal{J}^{A0},$$
$$\mathcal{J}^{A\mu} = \frac{1}{n\cdot\partial}\epsilon^{\mu\nu\alpha\beta}\partial_\nu n_\alpha j^A_\beta.$$

Since the classical fields $\mathcal{B}^{A\mu}$ satisfy the equation of motion

$$\partial\cdot(\partial\wedge\mathcal{B}^A)^\mu + m_A^2\mathcal{B}^{A\mu} = \mathcal{J}^{A\mu}, \tag{49}$$

the above equation becomes

$$\nabla\cdot\boldsymbol{H}^A(j) = -m_A^2\mathcal{B}^{A0}. \tag{50}$$

In the same way, we obtain

$$-\nabla\times\boldsymbol{E}^A(j) - \partial_0\boldsymbol{H}^A(j) = -m_A^2\boldsymbol{\mathcal{B}}^A. \tag{51}$$

In other words, because of the term $-m_A^2\mathcal{B}^{A\mu} = -m_A^2(\mathcal{B}^{A0}, \boldsymbol{\mathcal{B}}^A)$, the remaining two Maxwell equations are modified.

If we consider a model with the magnetic current $j^{A\mu}_{\rm mag} = (\rho^A_{\rm mag}, \boldsymbol{j}^A_{\rm mag})$, $\rho^A_{\rm mag}$ and $\boldsymbol{j}^A_{\rm mag}$ will appear in the right-hand sides of Eqs. (50) and (51), respectively. In the dual superconductor model there is the monopole field, and the static equation $-\nabla\times\boldsymbol{E}^A(j) = \boldsymbol{j}^A_{\rm mag}$ is often discussed [1,23]. In the present model there is no monopole field and no magnetic current originally. However, like the London equation in superconductivity, the relation $\boldsymbol{j}^A_{\rm mag} = -m_A^2\boldsymbol{\mathcal{B}}^A$ appears.

6.2 *Color flux tube*

It is expected that the color flux tube connects color charges. In Ref. [23], the color flux is studied using the dual superconductor model. From this flux and the equation $-\nabla\times\boldsymbol{E}^A(j) = \boldsymbol{j}_{\rm mag}$, the magnetic current is also investigated. In this subsection we consider the color flux tube.

Let us consider the electric flux between the charges $Q^A_{C_i}$ at $\boldsymbol{a} = (0, 0, a)$ and $\bar{Q}^A_{C_i}$ at $\boldsymbol{b} = (0, 0, b)$. We set $\boldsymbol{n} = (0, 0, 1)$, and assume that the mass m^A is approximately constant for $\rho > 1/\Lambda_{\rm c}$, where (ρ, θ, z) are the cylindrical coordinates. To study the static flux tube solution we set $\mathcal{B}^{A0} = 0$ and

$$\boldsymbol{\mathcal{B}}^A(\rho, \theta, z) \approx B(\rho)f(z)\boldsymbol{e}_\theta, \tag{52}$$

where the unit vectors are

$$\boldsymbol{e}_\rho = (\cos\theta, \sin\theta, 0), \qquad \boldsymbol{e}_{\boldsymbol{\theta}} = (-\sin\theta, \cos\theta, 0), \qquad \boldsymbol{e}_z = (0, 0, 1).$$

Substituting Eq. (52) into Eq. (49), we obtain

$$\left(\frac{\partial^2}{\partial\rho^2} + \frac{1}{\rho}\frac{\partial}{\partial\rho} - \frac{1}{\rho^2} - m_A^2\right) B(\rho)f(z) + B(\rho)f''(z) = \frac{1}{\partial_z}\frac{\partial}{\partial\rho} j_0^A. \tag{53}$$

Since $j_0^A = 0$ holds for $\rho > 0$, if we assume $f^{''}(z) \approx 0$ in the interval $b < z < a$, Eq. (53) reduces to

$$\left(\frac{\partial^2}{\partial\rho^2} + \frac{1}{\rho}\frac{\partial}{\partial\rho} - \frac{1}{\rho^2} - m_A^2\right) B(\rho) \approx 0$$

in the region ($\rho > 1/\Lambda_c$, $b < z < a$). The solution of this equation with $\lim_{\rho\to\infty} B(\rho) = 0$ is $B(\rho) = \lambda K_1(m_A\rho)$ [24], where λ is a constant and $K_n(X)$ is the modified Bessel function. So, we obtain

$$\boldsymbol{\mathcal{B}}^A \approx \lambda K_1(m_A\rho)f(z)\boldsymbol{e}_\theta. \tag{54}$$

Using Eq. (54) and the equality $XK_n'(X) + nK_n(X) = XK_{n-1}(X)$, the color electric field becomes

$$\boldsymbol{E}^A(j) = -\nabla\times\boldsymbol{\mathcal{B}}^A \approx m_A\lambda K_0(m^A\rho)f(z)\boldsymbol{e}_z + \lambda K_1(m_A\rho)f'(z)\boldsymbol{e}_\rho. \tag{55}$$

In the same way, if we apply the relations $XK_n'(X) - nK_n(X) = -XK_{n+1}(X)$ and $K_0'(X) = -K_1(X)$, we get

$$m^A\lambda\frac{\partial}{\partial\rho}K_0(m^A\rho)f(z)(\boldsymbol{e}_\rho\times\boldsymbol{e}_z) = -m_A^2\lambda K_1(m_A\rho)f(z)\boldsymbol{e}_\theta = -m_A^2\boldsymbol{\mathcal{B}}^A.$$

From this equation and Eq. (55), we obtain

$$-\nabla\times\boldsymbol{E}^A(j) = -m_A^2\boldsymbol{\mathcal{B}}^A + \lambda K_1(m^A\rho)f''(z)\boldsymbol{e}_\theta. \tag{56}$$

In the interval $b < z < a$, $f^{''}(z) \approx 0$ is assumed, and Eq. (56) becomes Eq. (51) with $\partial_0\boldsymbol{H}^A = 0$.

6.3 *Flux tube represented by* $\tilde{B}^{A\mu}$

Next, we restudy the flux tube by using the electric potential $\tilde{B}^{A\mu}$. In the static case, Eq. (46) becomes

$$\boldsymbol{E}(j)^A = -\nabla\tilde{B}^{A0} - \frac{\boldsymbol{n}}{n\cdot\partial}\Box\tilde{B}^{A0}. \tag{57}$$

From the equation of motion $\partial\cdot(\partial\wedge\tilde{B}^A)^\mu + m_A^2\tilde{B}^{A\mu} = j^{A\mu}$, $\tilde{B}^{A0}$ satisfies $\nabla^2\tilde{B}^{A0} - m_A^2\tilde{B}^{A0} = -j^{A0}$. If we can write $\tilde{B}^{A0} \approx D(\rho)h(z)$ approximately, this equation becomes

$$\left(\frac{\partial^2}{\partial\rho^2} + \frac{1}{\rho}\frac{\partial}{\partial\rho} - m_A^2\right) D(\rho)h(z) + D(\rho)h'(z) = -j^{A0}. \tag{58}$$

As in the previous subsection, we set $j^{A0} = 0$ for $\rho > 0$, and assume $h^{'}(z) \approx 0$ in the interval $b < z < a$. Then, Eq. (58) becomes

$$\left(\frac{\partial^2}{\partial\rho^2} + \frac{1}{\rho}\frac{\partial}{\partial\rho} - m_A^2\right) D(\rho) \approx 0.$$

Using the constant κ, the solution of this equation is $D(\rho) = \kappa K_0(m_A\rho)$. Since we choose $\boldsymbol{n} = (0, 0, 1)$, $\tilde{B}^{A0} \approx \kappa K_0(m_A\rho)h(z)$ gives

$$\begin{aligned} -\nabla\tilde{B}^{A0} &= m_A\kappa K_1(m_A\rho)h(z)\boldsymbol{e}_\rho - \kappa K_0(m_A\rho)h'(z)\boldsymbol{e}_z, \\ -\frac{\boldsymbol{n}}{n\cdot\partial}\Box\tilde{B}^{A0} &= \kappa m_A^2 K_0(m_A\rho)\frac{1}{\partial_z}h(z)\boldsymbol{e}_z + \kappa K_0(m_A\rho)h'(z)\boldsymbol{e}_z, \end{aligned} \tag{59}$$

and Eq. (57) becomes

$$\boldsymbol{E}(j)^A = \kappa m_A^2 K_0(m_A\rho)\frac{1}{\partial_z}h(z)\boldsymbol{e}_z + m_A\kappa K_1(m_A\rho)h(z)\boldsymbol{e}_\rho. \tag{60}$$

Comparing Eqs. (55) and (60), we can identify[4]

$$\kappa m_A = -\lambda, \qquad -\frac{1}{\partial_z}h(z) = f(z), \qquad -h(z) = f'(z).$$

So, $f(z)$ and $h(z)$ can be approximated by

$$f(z) \approx \theta(a-z) - \theta(b-z), \qquad h(z) \approx \delta(z-a) - \delta(z-b),$$

where $\theta(z)$ is the unit step function.

Thus, the electric potential

$$\tilde{B}^{A0} \approx -\frac{\lambda}{m_A}K_0(m_A\rho)\{\delta(z-a) - \delta(z-b)\} \tag{61}$$

produces the color electric flux

$$\boldsymbol{E}^A(j) \approx m_A\lambda K_0(m_A\rho)\{\theta(a-z) - \theta(b-z)\}\boldsymbol{e}_z \tag{62}$$

in the region ($\rho > 1/\Lambda_c$, $b < z < a$). The string part in Eq. (59) is responsible for this flux tube. The corresponding dual potential is

$$\boldsymbol{\mathcal{B}}^A \approx \lambda K_1(m_A\rho)\{\theta(a-z) - \theta(b-z)\}\boldsymbol{e}_\theta, \tag{63}$$

which also gives the flux in Eq. (62). This flux satisfies the extended Maxwell equation

$$-\nabla \times \boldsymbol{E}^A(j) \approx -m_A^2\boldsymbol{\mathcal{B}}^A, \tag{64}$$

where the magnetic current is $\boldsymbol{j}^A_{\rm mag} = -m_A^2\boldsymbol{\mathcal{B}}^A$.

We make a comment here. The lattice simulation shows that the $3q$ baryon is Y-shaped [20–22], and the solenoidal magnetic current exists [20]. In the present approach, the Y-type baryonic potential is free from infrared divergence, and it consists of three $q\bar{q}$ potentials. So, although the flux tube of $q\bar{q}$ is considered here, we can apply it to the Y-type $3q$ baryon. The flux tube of $q\bar{q}$ can exist between $\boldsymbol{r}_S$ and $\boldsymbol{r}_k$ ($k = 1, 2, 3$). The current $\boldsymbol{j}^A_{\rm mag} = -m_A^2\boldsymbol{\mathcal{B}}^A$ with Eq. (63), which has the solenoidal form, also appears.

7. Summary and comment

In the dual superconductor picture of quark confinement, monopole condensation produces the gluon mass. To realize this scenario, the dual Ginzburg–Landau model introduces the monopole field; its condensation, the gluon mass, and the static potential have been studied.

In Ref. [3], we considered another possibility to make the Abelian component of the gluon massive in the SU(2) gauge theory. The static potential was also studied [16]. In this paper, we extended this approach to the SU(3) gauge theory. In the nonlinear gauge of the Curci–Ferrari type, the quartic ghost interaction generates the ghost condensate $v^A = g\langle\varphi^A\rangle$ below the scale $\Lambda_{\rm QCD}$. The ghost loop with v^A gives rise to the tachyonic mass for the quantum part of the gluon. This tachyonic mass is removable by the gluon condensate $\langle A^a_\mu A^{a\mu}\rangle$. Since the classical part b^A_μ of the gluon has no tachyonic mass, the condensate $\langle A^a_\mu A^{a\mu}\rangle$ gives the mass m_A to this part. To study color confinement, the dual color electric potential $\mathcal{B}^A_\mu$, which is equivalent to the color electric potential $\tilde{B}^A_\mu$ with the string part $\Lambda_e^{A\mu\nu}$, was chosen as b^A_μ. Thus, the classical Lagrangian we used is $\mathcal{L}_{\rm cl}$ in Eq. (21).

[4]The minus sign comes from the choice that the electric string is in the negative z-direction; see Eq. (C4).

This Lagrangian becomes $\mathcal{L}_{jj}$ in Eq. (24), and it gives the static potential between the charges Q_a^A and Q_b^A with distance r. When r is small, the leading term is $V_Y^A(r)$ in Eq. (29). For large r, $V_L^A(\boldsymbol{r})$ in Eq. (30) is the main term. However, $V_L^A(\boldsymbol{r})$ contains the infrared divergence $V_{\rm IR}^A(r_t)$, which comes from the mass m_A and the electric string with infinite length. If the conditions $r_t = 0$ and $Q_a^A + Q_b^A = 0$ in Eq. (34) are fulfilled, $V_{\rm IR}^A(r_t)$ vanishes. In this case, $V_L^A(r)$ becomes the linear potential in Eq. (32).

We stress that the derivation of the Lagrangian $\mathcal{L}_{\rm cl}$ is based on the one-loop calculation. In addition, the constant sources K_A and $\mathcal{K}_\alpha$ are assumed. The mass m_A in Eq. (21) was also assumed to be constant below the cut-off $\Lambda_{\rm c}$ and to vanish above $\Lambda_{\rm c}$. These quantities must be determined. However, differently from the SU(2) case, there are many parameters in SU(3). We skipped the determination in this paper, and studied the consequences of the Lagrangian $\mathcal{L}_{\rm cl}$ and the potential $V_L^A(\boldsymbol{r})$.

In the $q\bar{q}$ case, the two conditions in Eq. (34) are satisfied, and the static potential $V_{q\bar{q}}(r)$ in Eq. (37) is obtained. In the $3q$ case, if the Δ-ansatz holds, the potential V_{3q}^Δ is given by Eq. (38). However, since the second condition of Eq. (34) is not fulfilled, the infrared divergence in Eq. (40) remains. Contrary to the Δ-ansatz, the Y-ansatz satisfies the two conditions. The potential V_{3qL}^Y in Eq. (41), which is free from the infrared divergence, is expected for large r.

Using the color electric potential $\tilde{B}_\mu^A$ and its dual potential $\mathcal{B}_\mu^A$, the color electric field $\boldsymbol{E}^A$ and the magnetic field $\boldsymbol{H}^A$ were investigated. Although they satisfy the two Maxwell equations in Eq. (48), because of the mass m_A, the remaining two equations are modified as Eqs. (50) and (51). In the static case, Eq. (51) becomes $-\nabla \times \boldsymbol{E}^A(j) = -m_A^2 \boldsymbol{\mathcal{B}}^A$. In the dual Ginzburg–Landau model, which contains the monopole field, the equation $-\nabla \times \boldsymbol{E}^A(j) = \boldsymbol{j}_{\rm mag}$ has been discussed. In our model, although there is no monopole field, the current $-m_A^2 \boldsymbol{\mathcal{B}}^A$ plays the role of the magnetic current $\boldsymbol{j}_{\rm mag}$.

It is expected that the color flux tube exists between color charges. The dual electric potential $\boldsymbol{\mathcal{B}}^A$ in Eq. (63) produces the electric flux $\boldsymbol{E}^A(j)$ in Eq. (62), and they satisfy Eq. (64). Namely, without the monopole field, the flux tube $\boldsymbol{\mathcal{B}}^A$ leads to the magnetic current $\boldsymbol{j}_{\rm mag} = -m_A^2 \boldsymbol{\mathcal{B}}^A$. The corresponding electric potential $\tilde{B}^{A0}$ is presented in Eq. (61). The string part, Eq. (59), is the origin of the flux tube in Eq. (62).

Comparing the SU(3) case with the SU(2) case in Ref. [3], there are some differences. For example, as stated in Sect. 3, although the condensate of the diagonal component $\langle A^{3\mu} A_\mu^3 \rangle$ vanishes in SU(2), the condensates $\langle A^{A\mu} A_\mu^A \rangle$ ($A = 3, 8$) exist in SU(3). Equation (18) shows there are two different mass scales, $\sqrt{5}m/2$ and $\sqrt{3}m/2$, and the classical electric potentials $\tilde{B}_\mu^3$ and $\tilde{B}_\mu^8$ have different masses, whereas the tachyonic mass term in SU(2) has one scale, m.

Since we have not determined the parameters yet, it is difficult to study the differences between SU(2) and SU(3) concretely. In Ref. [25], the differences are discussed. One of the issues is the type of the dual superconductivity. Investigating the electric flux, it was concluded that the SU(3) theory is type-I, whereas the SU(2) theory is weak type-I or on the border between type-I and type-II. In Appendix E, assuming the phenomenological Lagrangian for the order parameters $\mathcal{G}^\alpha$ and G^A, we consider the type of dual superconductivity in the present model. Because of the condensate $\langle A^{8\mu} A_\mu^8 \rangle$ and the two mass scales $\sqrt{5}m/2$ and $\sqrt{3}m/2$, the value of the Ginzburg–Landau parameter for SU(3) may become smaller than that for SU(2).

Funding

Open Access funding: SCOAP[3].

Appendix A. $\Lambda_{\rm QCD}$ and α_2

In the momentum region $\mu \geq \Lambda_{\rm QCD}$, as the effective potential $V(\varphi)$ in Eq. (5) gives $v = 0$, we consider the Wilsonian effective action

$$\begin{aligned}\Gamma_{[\mu,\Lambda]} &= \int d^4x \left\{ \sum_{\alpha=1}^{3} \left(\frac{(g\vec{\epsilon}_\alpha \cdot \vec{\varphi})^2}{3\alpha_2 g^2} - \int_\mu^\Lambda \frac{d^4k}{(2\pi)^4} \ln\left[(-k^2)^2 + (g\vec{\epsilon}_\alpha \cdot \vec{\varphi})^2\right] \right) \right\} \\ &= \int d^4x \left\{ \sum_{\alpha=1}^{3} \left(\frac{(g\vec{\epsilon}_\alpha \cdot \vec{\varphi})^2}{3\alpha_2 g^2} - \int_\mu^\Lambda \frac{d^4k}{(2\pi)^4} \frac{(g\vec{\epsilon}_\alpha \cdot \vec{\varphi})^2}{(-k^2)^2} + \cdots \right) \right\} \\ &= \int d^4x \left\{ \sum_{\alpha=1}^{3} \left(\frac{1}{3\alpha_2 g^2} - \frac{1}{8\pi^2} \ln \frac{\Lambda}{\mu} \right) (g\vec{\epsilon}_\alpha \cdot \vec{\varphi})^2 + \cdots \right\}. \end{aligned} \tag{A1}$$

If $\bar{g}$ and $\bar{\alpha}_2$ represent the quantities at the scale μ, Eq. (A1) implies

$$\frac{1}{\bar{\alpha}_2 \bar{g}^2} = \frac{1}{\alpha_2 g^2} - \frac{3}{8\pi^2} \ln \frac{\Lambda}{\mu} = -\frac{3}{8\pi^2} \ln \frac{\mu_0}{\mu}, \qquad \mu_0 = \Lambda \exp\left(-\frac{8\pi^2}{3\alpha_2 g^2} \right). \tag{A2}$$

From Eq. (A2), we obtain

$$\mu \frac{\partial}{\partial \mu} \bar{\alpha}_2 \bar{g}^2 = -\frac{3}{8\pi^2} (\bar{\alpha}_2 \bar{g}^2)^2. \tag{A3}$$

Since $\bar{g}$ satisfies

$$\mu \frac{\partial}{\partial \mu} \bar{g} = -\frac{\beta_0}{(4pi)^2} \bar{g}^3, \qquad \beta_0 = \frac{11}{3} N \tag{A4}$$

at the one-loop level, Eqs. (A3) and (A4) lead to

$$\mu \frac{\partial}{\partial \mu} \bar{\alpha}_2 = \frac{\bar{\alpha}_2 \bar{g}^2}{8\pi^2} (\beta_0 - 3\bar{\alpha}_2).$$

Namely, $\alpha_2 = \beta_0/3$ is the ultraviolet fixed point [7,8], i.e.,

$$\lim_{\mu \to \Lambda} \bar{\alpha}_2 = \alpha_2 = \frac{\beta_0}{3}.$$

Substituting this α_2, we find $\mu_0 = \Lambda \exp(-8\pi^2/\beta_0 g^2) = \Lambda_{\rm QCD}$ [7,8].

Appendix B. Tachyonic gluon masses

B.1 $\left\langle A_\mu^A A_\nu^B \right\rangle^{-1}$

We consider the diagrams in Fig. B1(a) in the limit $p \to 0$, where p is the external momentum. The ghost propagators in Eq. (8) and the interaction

$$\sum_{A=3,8} \left[-g A^{A\mu} \sum_{\alpha=1}^{3} \epsilon_\alpha^A \left\{ (\partial_\mu \bar{C}^\alpha) C^{-\alpha} - (\partial_\mu \bar{C}^{-\alpha}) C^\alpha \right\} \right]$$

in Eq. (9) give the integral

$$\sum_{\alpha=1}^{3} g^2 \epsilon_\alpha^A \epsilon_\alpha^B i \int \frac{d^4k}{(2\pi)^4} \left\{ \frac{k_\mu k_\nu \left(-k^2 + i\epsilon_\alpha^3 v\right)^2}{[k^4 + \left(\epsilon_\alpha^3 v\right)^2]^2} + (v \to -v) \right\}. \tag{B1}$$

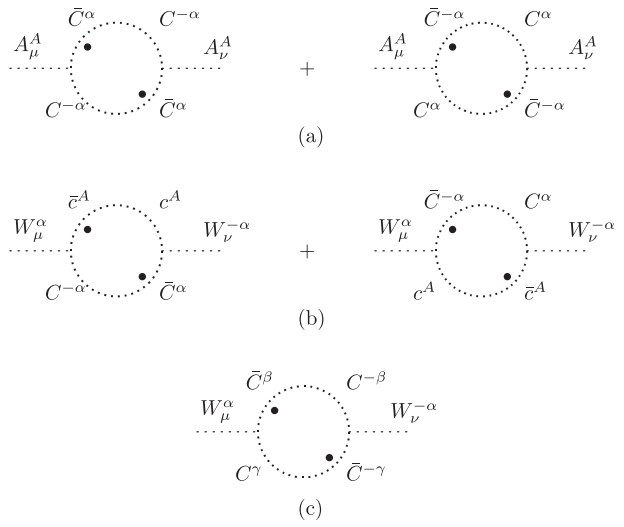

Fig. B1. The diagrams that contribute to the tachyonic gluon masses.

Performing the Wick rotation and neglecting v-independent terms, we obtain

$$\begin{aligned} & i\int \frac{d^4k}{(2\pi)^4}\left\{\frac{k_\mu(-k^2+i\eta v)k_\nu(-k^2+i\xi v)}{[k^4+(\eta v)^2][k^4+(\xi v)^2]}+(v\to -v)\right\} \\ & \quad = 2i\int \frac{d^4k}{(2\pi)^4}\frac{k_\mu k_\nu(k^4-\eta\xi v^2)}{[k^4+(\eta v)^2][k^4+(\xi v)^2]} = -\frac{v}{64\pi}g_{\mu\nu}\frac{\eta^2+\xi^2+\eta\xi+|\eta\xi|}{|\eta|+|\xi|}. \end{aligned} \tag{B2}$$

If we apply this formula, we find that Eq. (B1) becomes

$$-\frac{g^2 v}{32\pi}g_{\mu\nu}\epsilon^A_\alpha\epsilon^B_\alpha|\epsilon^3_\alpha|.$$

Using the values of ϵ^A_α in Eq. (2), we obtain

$$-\frac{5}{2}g_{\mu\nu}m^2 \quad (A=B=3), \qquad -\frac{3}{2}g_{\mu\nu}m^2 \quad (A=B=8), \qquad m^2=\frac{g^2 v}{64\pi}. \tag{B3}$$

B.2 $\langle W^\alpha_\mu W^{-\alpha}_\nu\rangle^{-1}$

The diagrams in Fig. B1(b), which come from the interaction

$$\sum_{A=3,8}\left[g(\partial_\mu\bar{c}^A)\sum_{\alpha=1}^{3}\epsilon^A_\alpha(W^{\alpha\mu}C^{-\alpha}-W^{-\alpha\mu}C^{\alpha})-g\sum_{\alpha=1}^{3}\epsilon^A_\alpha\left\{W^{\alpha\mu}(\partial_\mu\bar{C}^{-\alpha})-W^{-\alpha\mu}(\partial_\mu\bar{C}^{\alpha})\right\}c^A\right],$$

give the integral

$$\sum_{A=3,8}g^2\left(\epsilon^A_\alpha\right)^2 i\int\frac{d^4k}{(2\pi)^4}\left\{\frac{k_\mu k_\nu(-k^2)\left(-k^2+i\epsilon^3_\alpha v\right)}{k^4\left[k^4+\left(\epsilon^3_\alpha v\right)^2\right]}+(v\to -v)\right\} = -\sum_{A=3,8}\frac{g^2 v}{64\pi}g_{\mu\nu}\left(\epsilon^A_\alpha\right)^2|\epsilon^3_\alpha|.$$

Using the values of ϵ^A_α in Eq. (2), we obtain

$$-g_{\mu\nu}m^2 \quad (\alpha=1), \qquad -\frac{1}{2}g_{\mu\nu}m^2 \quad (\alpha=2,3). \tag{B4}$$

In the same way, the interaction

$$\sum_{(\alpha,\beta,\gamma)}\mathrm{sgn}(\gamma)\frac{g}{\sqrt{2}}\epsilon_{\alpha\beta\gamma}(\partial_\mu\bar{C}^\alpha)C^\beta W^{\gamma\mu}$$

in Eq. (9) produces the diagram in Fig. B1(c). Applying the formula in Eq. (B2), this diagram gives

$$\frac{g^2}{2} i \int \frac{d^4k}{(2\pi)^4} \left\{ \frac{k_\mu k_\nu \left(-k^2 + i\epsilon_\beta^3 v\right)\left(-k^2 - i\epsilon_\gamma^3 v\right)}{\left[k^4 + \left(\epsilon_\beta^3 v\right)^2\right]\left[k^4 + \left(\epsilon_\gamma^3 v\right)^2\right]} + (v \to -v) \right\}$$

$$= -\frac{g^2 v}{64\pi} g_{\mu\nu} \frac{\left(\epsilon_\beta^3\right)^2 + \left(\epsilon_\gamma^3\right)^2 - \epsilon_\beta^3 \epsilon_\gamma^3 + \left|\epsilon_\beta^3 \epsilon_\gamma^3\right|}{\left|\epsilon_\beta^3\right| + \left|\epsilon_\gamma^3\right|} \qquad (\beta < \gamma,\ \alpha \neq \beta, \gamma). \tag{B5}$$

From the values of ϵ_α^A in Eq. (2), we find that Eq. (B5) becomes

$$-\frac{1}{4} g_{\mu\nu} m^2 \quad (\alpha = 1), \qquad -\frac{3}{4} g_{\mu\nu} m^2 \quad (\alpha = 2, 3). \tag{B6}$$

Thus, by summing Eqs. (B4) and (B6), we obtain

$$-\frac{5}{4} g_{\mu\nu} m^2 \qquad (\alpha = 1, 2, 3). \tag{B7}$$

Appendix C. Example of the electric potential and its dual potential

In this appendix we present an example of the massless electric potential $\tilde{B}_\mu^A$ and its dual potential $\mathcal{B}_\mu^A$ for a color electric charge Q^A. The color electric current is $j^{A\mu} = Q^A \delta(x)\delta(y)\delta(z) g^{\mu 0}$, and the electric potential

$$\tilde{B}^{A\mu} = \frac{Q^A}{4\pi} \frac{1}{r} g^{\mu 0}, \qquad r = \sqrt{x^2 + y^2 + z^2}, \tag{C1}$$

satisfies the equation of motion $\partial_\mu (\partial \wedge \tilde{B}^A)^{\mu\nu} - j^{A\nu} = 0$.

The dual electric potential that corresponds to Eq. (C1) is

$$\mathcal{B}^{A\mu} = \frac{Q^A}{4\pi} \frac{z - r}{r\rho^2} (0, -y, x, 0), \qquad \rho = \sqrt{x^2 + y^2}. \tag{C2}$$

This field fulfills the equation of motion

$$\partial_\mu (\partial \wedge \mathcal{B}^A)^{\mu\nu} + \epsilon^{\nu\alpha\mu\beta} \frac{n_\alpha \partial_\mu}{n \cdot \partial} j_\beta^A = 0,$$

and gives the color electric field

$$E^{Ai} = -\epsilon^{i0jk} \partial_j \mathcal{B}_k^A = \frac{Q^A}{4\pi} \frac{x^i}{r^3} + \delta_3^i Q^A \delta(x)\delta(y)\theta(-z), \tag{C3}$$

where $\theta(z)$ is the unit step function, and $(\partial_x^2 + \partial_y^2) \ln \rho = 2\pi \delta(x)\delta(y)$ has been used.

From Eq. (C1), we get

$$(\partial \wedge \tilde{B}^A)^{i0} = \frac{Q^A}{4\pi} \frac{x^i}{r^3}.$$

The string part in Eq. (C3) comes from $\Lambda_e^{A\mu\nu}$ in Eq. (25). To choose the electric string in the negative z-direction, we use

$$\frac{1}{\partial_z} \delta(z) = -\theta(-z). \tag{C4}$$

Then, Eq. (C1) gives

$$\left(\Lambda_e^A\right)^{i0} = -\delta_3^i \frac{1}{\partial_z} \partial_j (\partial \wedge \tilde{B}^A)^{j0} = \delta_3^i Q^A \delta(x)\delta(y)\theta(-z),$$

where $\nabla^2 (1/r) = -4\pi \delta(\boldsymbol{r})$ has been used. The sum $(\partial \wedge \tilde{B}^A)^{i0} + (\Lambda_e^A)^{i0}$ reproduces Eq. (C3).

Appendix D. The potentials $V_Y^A(r)$ and $V_L^A(r)$

D.1 $V_Y^A(r)$

By subtracting r-independent terms, which contain ultraviolet divergence, V_Y^A in Eq. (27) becomes

$$\int \frac{d^3q}{(2\pi)^3} \frac{Q_a^A Q_b^A}{q^2 + m_A^2} e^{i\boldsymbol{q}\cdot\boldsymbol{r}}.$$

If the mass m_A disappears above some scale Λ_c, this potential can be written as

$$\int_0^{\Lambda_c} dq W(\boldsymbol{q}, m, r) + \int_{\Lambda_c}^{\infty} dq W(\boldsymbol{q}, 0, r) = \int_0^{\infty} dq W(\boldsymbol{q}, 0, r) + \int_0^{\Lambda_c} dq \{W(\boldsymbol{q}, m, r) - W(\boldsymbol{q}, 0, r)\}.$$

The first term on the right-hand side gives the Coulomb potential, which contributes mainly in the small-r region. When r becomes large, the second term weakens the effect of the first term. After performing the integration, we obtain [16]

$$V_Y^A(r) = Q_a^A Q_b^A \left(\frac{1}{4\pi r} - \frac{m_A^2}{2\pi^2} \int_0^{\Lambda_c} dq \frac{\sin qr}{qr} \frac{1}{q^2 + m_A^2} \right). \tag{D1}$$

We note that this potential satisfies

$$\lim_{\Lambda_c \to \infty} V_Y^A(r) = \frac{Q_a^A Q_b^A}{4\pi} \frac{e^{-m^A r}}{r}. \tag{D2}$$

In the usual approach [2,12–14], the cut-off is not taken into account, and $V_Y^A(r)$ becomes the Yukawa potential, Eq. (D2).

D.2 $V_L^A(\boldsymbol{r})$

When $m^A = 0$, the potential $V_L^A(\boldsymbol{r})$ in Eq. (28) vanishes. So, differently from $V_Y^A(r)$, the momentum region $q = |\boldsymbol{q}| \leq \Lambda_c$ contributes to $V_L^A(r)$. Let us write $\boldsymbol{r} = (r_n, \boldsymbol{r}_t)$, and choose $\boldsymbol{n}$ as $r_n = \boldsymbol{r} \cdot \boldsymbol{n} \geq 0$. The vector $\boldsymbol{r}_t$ satisfies $\boldsymbol{r}_t \cdot \boldsymbol{n} = 0$, and $r_t = |\boldsymbol{r}_t|$. Similarly, we write $\boldsymbol{q} = (q_n, \boldsymbol{q}_t)$, and use the spherical coordinates $q_n = q\cos\theta$, $q_{t1} = q\sin\theta\cos\varphi$, $q_{t2} = q\sin\theta\sin\varphi$ ($q < \Lambda_c$, $0 \leq \theta \leq \pi$, $0 \leq \varphi < 2\pi$), where q_{t1} is chosen to satisfy $\boldsymbol{q}_t \cdot \boldsymbol{r}_t = q\sin\theta\cos\varphi r_t$.

Now we consider the integral

$$\int \frac{d^3q}{(2\pi)^3} \frac{e^{i\boldsymbol{q}\cdot\boldsymbol{r}}}{q_n^2 \left(q^2 + m_A^2\right)} \tag{D3}$$

in V_L^A. It becomes

$$\int_0^{\Lambda_c} \frac{dq}{(2\pi)^3} \int_0^{\pi} d\theta \sin\theta \int_0^{2\pi} d\varphi \frac{e^{iqr_n\cos\theta} e^{iqr_t\sin\theta\cos\varphi}}{\cos^2\theta \left(q^2 + m_A^2\right)}. \tag{D4}$$

By changing the variable θ to $u = \cos\theta$, we get

$$\int_0^{\pi} d\theta \sin\theta \frac{e^{iqr_n\cos\theta} e^{iqr_t\sin\theta\cos\varphi}}{\cos^2\theta} = \int_{-1}^{1} du \frac{e^{iqr_n u} e^{iqr_t\sqrt{1-u^2}\cos\varphi}}{u^2},$$

which diverges at $u = 0$. If we choose the path C in Fig. D1, the integral

$$\int_C dz \frac{e^{izqr_n} e^{iqr_t\sqrt{1-z^2}\cos\varphi}}{z^2} = 0,$$

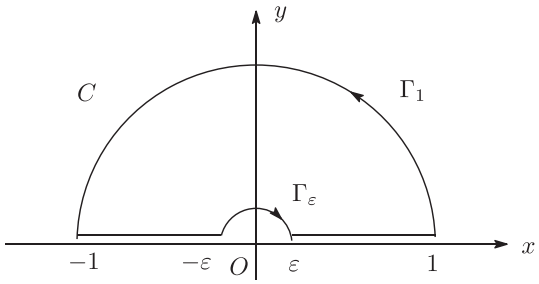

Fig. D1. The path C on the complex plane.

leading to

$$\mathcal{P}\int_{-1}^{1} du \frac{e^{iqr_n u} e^{iqr_t\sqrt{1-u^2}\cos\varphi}}{u^2} = I_{\Gamma_\varepsilon} + I_{\Gamma_1}, \qquad I_{\Gamma_\varepsilon} = -\int_{\Gamma_\varepsilon} dz \frac{e^{iqr_n z} e^{iqr_t\sqrt{1-z^2}\cos\varphi}}{z^2},$$
$$I_{\Gamma_1} = -\int_{\Gamma_1} dz \frac{e^{iqr_n z} e^{iqr_t\sqrt{1-z^2}\cos\varphi}}{z^2}, \tag{D5}$$

where $\mathcal{P}$ means the Cauchy principal value. To calculate I_{Γ_ε} we use the variable $z = \varepsilon e^{i\phi}$, and take the limit $\varepsilon \to +0$. Then it becomes

$$I_{\Gamma_\varepsilon} = \lim_{\varepsilon\to+0}\left\{\frac{2}{\varepsilon} - \pi q r_n + O(\varepsilon)\right\} e^{iqr_t\cos\varphi}. \tag{D6}$$

Similarly, by setting $z = e^{i\phi}$ in I_{Γ_1}, we find

$$I_{\Gamma_1} = -i\int_0^\pi d\phi e^{-i\phi} e^{iqr_n e^{i\phi}} e^{iqr_t\cos\varphi\sqrt{1-e^{2i\phi}}}. \tag{D7}$$

We note that Eq. (D7) satisfies

$$\left|I_{\Gamma_1}\right| \le \int_0^\pi d\phi e^{-qr_n\sin\phi} e^{-qr_t\cos\varphi\sqrt{2\sin\phi}\{\sin(2\phi-\pi)/4\}} \le \pi e^{qr_t/2}. \tag{D8}$$

If we substitute Eqs. (D5), (D6), and (D7) into Eq. (D4), we find

$$\int\frac{d^3q}{(2\pi)^3}\frac{e^{i\boldsymbol{q}\cdot\boldsymbol{r}}}{q_n^2\left(q^2+m_A^2\right)} = \frac{1}{2\pi^2\varepsilon}H(m_A,\Lambda_c,r_t) - \frac{1}{4\pi}K_0(m_A r_t,\Lambda_c)r_n + \mathcal{I}(m_A,\Lambda_c,r_n,r_t),$$
$$\mathcal{I}(m_A,\Lambda_c,r_n,r_t) = \int_0^{\Lambda_c}\frac{dq}{(2\pi)^3}\frac{1}{q^2+m_A^2}\int_0^{2\pi} d\varphi\, I_{\Gamma_1}, \tag{D9}$$

where, using the Bessel function $J_0(qr_t)$, $H(m_A,\Lambda_c,r_t)$ and $K_0(m_A r_t,\Lambda_c)$ are defined by

$$H(m_A,\Lambda_c,r_t) = \int_0^{\Lambda_c} dq\frac{1}{q^2+m_A^2}J_0(qr_t),$$
$$K_0(m_A r_t,\Lambda_c) = \int_0^{\Lambda_c} dq\frac{q}{q^2+m_A^2}J_0(qr_t),$$
$$J_0(qr_t) = \frac{1}{2\pi}\int_0^{2\pi} d\varphi e^{iqr_t\cos\varphi}. \tag{D10}$$

These functions satisfy

$$H(m_A, \Lambda_c, 0) = \frac{1}{m_A}\tan^{-1}\frac{\Lambda_c}{m_A},$$
$$\lim_{r_t\to+0} K_0(m_A r_t, \Lambda_c) = \frac{1}{2}\ln\left(\frac{\Lambda_c^2+m_A^2}{m_A^2}\right),$$
$$K_0(m_A r_t) = \lim_{\Lambda_c\to\infty} K_0(m_A r_t, \Lambda_c), \tag{D11}$$

where $K_0(m_A r_t)$ is the modified Bessel function. The term $\mathcal{I}$ in Eq. (D9) has the properties

$$\mathcal{I}(m_A, \Lambda_c, 0, 0) = -\frac{1}{2\pi^2}\frac{1}{m_A}\tan^{-1}\frac{\Lambda_c}{m_A}, \tag{D12}$$

$$|\mathcal{I}(m_A, \Lambda_c, r_n, r_t)| \le \frac{1}{8\pi^3}\int_0^{\Lambda_c} dq\frac{1}{q^2+m_A^2}\int_0^{2\pi} d\varphi\,|I_{\Gamma_1}| \le \frac{1}{4\pi}\int_0^{\Lambda_c} dq\frac{1}{q^2+m_A^2}e^{qr_t/2}$$
$$\to \frac{1}{4\pi m_A}\tan^{-1}\frac{\Lambda_c}{m_A} \qquad (r_t\to 0). \tag{D13}$$

Thus, using Eqs. (D9), (D11), and (D12), the potential V_L^A in Eq. (28) becomes

$$V_L^A(\boldsymbol{r}) = V_{\rm IR}^A(r_t) - \frac{Q_a^A Q_b^A m_A^2}{4\pi}K_0(m_A r_t, \Lambda_c)r_n$$
$$+ m_A^2\left\{-\frac{\left(Q_a^A\right)^2+\left(Q_b^A\right)^2}{2}\frac{1}{2\pi^2 m_A}\tan^{-1}\frac{\Lambda_c}{m_A} + Q_a^A Q_b^A\mathcal{I}(m_A, \Lambda_c, r_n, r_t)\right\}, \tag{D14}$$

$$V_{\rm IR}^A(r_t) = \frac{m_A^2}{2\pi^2\varepsilon}\left\{\frac{\left(Q_a^A\right)^2+\left(Q_b^A\right)^2}{2}\frac{1}{m_A}\tan^{-1}\frac{\Lambda_c}{m_A} + Q_a^A Q_b^A H(m_A, \Lambda_c, r_t)\right\}. \tag{D15}$$

We note that the first term has the infrared divergence $1/\varepsilon$, and the second term leads to the linear potential. When $r_t\to 0$, as Eq. (D13) shows, the last term does not depend on r_n so much. Therefore, in Sect. 4 we study the potential $V_L^A(r)$ based on the first and second terms in Eq. (D14).

Here, we add a comment. Usually, the ultraviolet cut-off Λ_c is introduced as $|q_t| < \Lambda_c$ [3,12–14]. The domain of integration is $|q_n| < \infty$ and $|q_t| < \Lambda_c$. The infrared divergence and the linear potential come from the region with $|q_n| = \varepsilon_n$ ($\varepsilon_n \ll 1$). In this article, as $m_A = 0$ above Λ_c, the domain of integration is $q = |\boldsymbol{q}| < \Lambda_c$. The infrared divergence and the linear potential result from $\cos\theta = \varepsilon$ ($\varepsilon \ll 1$). Although the linear potential in these references coincides with that in this article, the coefficient of the infrared divergent term is different. From $q_n = q\cos\theta$, we find that ε_n is related to ε as $\varepsilon_n = q\varepsilon$. By using this relation, the infrared divergence in Ref. [3] becomes Eq. (D15).

Appendix E. Type of dual superconductivity

In the Ginzburg–Landau (GL) theory of superconductivity, the space dependence of an order parameter Φ is considered (see, e.g., Ref. [26]). To see the coherence length, the x-dependence is introduced as $\Phi(x) = \Phi f(x)$ with $f(0) = 0$ and $\lim_{x\to\infty} f(x) = 1$. From the phenomenological Lagrangian for $\Phi(x)$, the function $f(x)$ satisfies

$$\xi^2\frac{d^2 f(x)}{dx^2} = -\left[1-\{f(x)\}^2\right]f(x). \tag{E1}$$

The solution is $f(x) = \tanh \frac{x}{\sqrt{2}\xi}$, with ξ the coherence length. The penetration depth λ is determined by the mass of the magnetic field, and the parameter $\kappa = \lambda/\xi$ is called the GL parameter. When $\kappa < 1/\sqrt{2}$ ($\kappa > 1/\sqrt{2}$), the superconductor is called type-I (type-II).

In the following subsections, under some assumptions, we consider the coherence length and the GL parameter in the present model.

E.1 SU(2) case

First, we consider the SU(2) case. In Refs. [2,3], we showed that the tachyonic mass term for the off-diagonal component $A^{\pm}_{\mu} = (A^1_{\mu} \pm A^2_{\mu})/\sqrt{2}$ is $-m^2 A^+_{\mu} A^{-\mu}$, and the interaction in $-F^2_{\mu\nu}/4$ contains the term $-g^2(A^+_{\mu}A^{-\mu})^2/2$. From these terms, we obtain the gauge field condensate $\mathcal{G} = \langle A^+_{\mu}A^{-\mu}\rangle^{(0)} = -m^2/g^2$ at the one-loop level. This condensate makes the classical U(1) field b_{μ} massive. As its mass term becomes $m^2 b_{\mu} b^{\mu}$, the penetration depth of b_{μ} is $\lambda = 1/\sqrt{2}m$.

Now we consider the spatial behavior of the condensate $\mathcal{G}$. Since $\mathcal{G}$ has mass dimension 2, we assume its x-dependence is expressed by $\mathcal{G}(x) = \left\{\sqrt{\mathcal{G}} f(x)\right\}^2$ with $f(0) = 0$ and $\lim_{x\to\infty} f(x) = 1$. As $\mathcal{G}(x)$ depends on x, we introduce the kinetic energy in the form $\left\{\sqrt{\mathcal{G}} f'(x)\right\}^2$. Thus, using this kinetic term, the above tachyonic mass term, and the interaction, we assume the following phenomenological Lagrangian for $\mathcal{G}(x)$:

$$\mathcal{L}_{2\mathrm{ph}} = \eta^2 \mathcal{G} \left\{\frac{df(x)}{dx}\right\}^2 - m^2 \mathcal{G} \{f(x)\}^2 - \frac{g^2}{2}\left[\mathcal{G}\{f(x)\}^2\right]^2,$$

where η is a parameter to adjust the effect of the assumed kinetic term. This Lagrangian leads to

$$\eta^2 \frac{d^2 f(x)}{dx^2} = -m^2 f(x) - g^2 \mathcal{G}\{f(x)\}^3 = -m^2\left[1 - \{f(x)\}^2\right] f(x),$$

where $\mathcal{G} = -m^2/g^2$ has been used. This equation implies $\xi = \eta/m$. From $\lambda = 1/\sqrt{2}m$ and $\xi = \eta/m$, we find $\kappa = 1/\sqrt{2}\eta$. If $\eta \simeq 1$, it implies the border between type-I and type-II.

E.2 SU(3) case

As in the SU(2) case, we assume the x-dependent order parameters $\mathcal{G}^{\alpha}(x) = \left\{\sqrt{\mathcal{G}^{\alpha}} f_{\alpha}(x)\right\}^2$ ($\alpha = 1, 2, 3$) and $G^A(x) = \left\{\sqrt{G^A}\phi_A(x)\right\}^2$ ($A = 3, 8$). Using the tachyonic mass terms in Eq.(11), the interaction terms in Eq. (12), and the assumed kinetic terms with the same parameter η, we consider the phenomenological Lagrangian

$$\begin{aligned}
\mathcal{L}_{3\mathrm{ph}} = &\sum_{\alpha=1}^{3} \mathcal{G}^{\alpha}\left\{\eta^2\left(\frac{df_{\alpha}}{dx}\right)^2 - \frac{5}{4}m^2 (f_{\alpha})^2\right] + \sum_{A=3,8} G^A \left\{\eta^2\left(\frac{d\phi_A}{dx}\right)^2 - \frac{m_A^2}{2}(\phi_A)^2\right\} \\
&- \frac{g^2}{2}\sum_{\alpha=1}^{3}(\mathcal{G}^{\alpha})^2\left\{(f_{\alpha})^2\right\}^2 - \frac{g^2}{4}\sum_{\alpha\neq\beta}\mathcal{G}^{\alpha}\mathcal{G}^{\beta}(f_{\alpha})^2(f_{\beta})^2 \\
&- g^2\left\{G^3\mathcal{G}^1(\phi_3)^2(f_1)^2 + \frac{1}{4}\left\{G^3(\phi_3)^2 + 3G^8(\phi_8)^2\right\}\sum_{\alpha=2}^{3}\mathcal{G}^{\alpha}(f_{\alpha})^2\right\}.
\end{aligned}$$

From $\mathcal{L}_{3\mathrm{ph}}$, we obtain the equations for $f_2(x)$ and $\phi_8(x)$:

$$\begin{aligned}
\eta^2\frac{d^2 f_2}{dx^2} = &-\frac{5m^2}{4} f_2 \\
&- g^2\left[\mathcal{G}^2(f_2)^2 + \frac{1}{2}\left\{\mathcal{G}^1(f_1)^2 + \mathcal{G}^3(f_3)^2\right\} + \frac{1}{4}\left\{G^3(\phi_3)^2 + 3G^8(\phi_8)^2\right\}\right] f_2, \quad \text{(E2)}
\end{aligned}$$

$$\eta^2\frac{d^2\phi_8}{dx^2} = -\frac{3m^2}{4}\phi_8 - \frac{3g^2}{4}\left\{\mathcal{G}^2(f_2)^2 + \mathcal{G}^3(f_3)^2\right\}\phi_8. \tag{E3}$$

If we assume the relation $f_\alpha(x) \simeq \phi_A(x)$ ($\alpha = 1, 2, 3$, $A = 3, 8$), these equations become

$$\eta^2\frac{d^2 f_2}{dx^2} \simeq -\frac{5m^2}{4}\left\{1 - (f_2)^2\right\} f_2, \tag{E4}$$

$$\eta^2\frac{d^2\phi_8}{dx^2} \simeq -\frac{3m^2}{4}\left\{1 - (\phi_8)^2\right\}\phi_8, \tag{E5}$$

where Eqs. (13) and (15) have been used. In the same way, we find that f_1, f_3, and ϕ_3 also satisfy Eq. (E4). Therefore, comparing these equations with Eq. (E1), we find

$$f_\alpha(x) \simeq \phi_3(x) \simeq \tanh\frac{x}{\sqrt{2}\xi_3}, \quad \xi_3 = \frac{2\eta}{\sqrt{5}m}, \quad \phi_8(x) \simeq \tanh\frac{x}{\sqrt{2}\xi_8}, \quad \xi_8 = \frac{2\eta}{\sqrt{3}m}. \tag{E6}$$

Equation (E6) shows that we have to modify Eqs. (E4) and (E5) to satisfy the relation $f_\alpha \simeq \phi_3 \neq \phi_8$. If we use this relation, Eqs. (E2) and (E3) become

$$\eta^2\frac{d^2 f_2}{dx^2} \simeq -\frac{5m^2}{4}\left\{1 - (f_2)^2\right\} f_2 - \frac{3g^2}{4}G^8\left\{(\phi_8)^2 - (f_2)^2\right\} f_2, \tag{E7}$$

$$\eta^2\frac{d^2\phi_8}{dx^2} \simeq -\frac{3m^2}{4}\left\{1 - (\phi_8)^2\right\}\phi_8 - \frac{3g^2}{2}\mathcal{G}^2\left\{(f_2)^2 - (\phi_8)^2\right\}\phi_8, \tag{E8}$$

where Eqs. (13) and (15) have been used again. Now we use Eq. (16), and rewrite the second terms on the right-hand side as

$$-\frac{3g^2}{4}G^8\left\{(\phi_8)^2 - (f_2)^2\right\} f_2 = -\frac{m^2}{16}\delta_2(x)\left\{1 - (f_2)^2\right\} f_2, \qquad \delta_2(x) = \frac{(f_2)^2 - (\phi_8)^2}{1 - (f_2)^2},$$

$$-\frac{3g^2}{2}\mathcal{G}^2\left\{(f_2)^2 - (\phi_8)^2\right\}\phi_8 = \frac{3m^2}{4}\delta_8(x)\left\{1 - (\phi_8)^2\right\}\phi_8, \qquad \delta_8(x) = \frac{(f_2)^2 - (\phi_8)^2}{1 - (\phi_8)^2}.$$

Then, Eqs. (E7) and (E8) become

$$\eta^2\frac{d^2 f_2}{dx^2} \simeq -\frac{5m^2}{4}\left\{1 + \frac{\delta_2(x)}{20}\right\}\left\{1 - (f_2)^2\right\} f_2, \tag{E9}$$

$$\eta^2\frac{d^2\phi_8}{dx^2} \simeq -\frac{3m^2}{4}\left\{1 - \delta_8(x)\right\}\left\{1 - (\phi_8)^2\right\}\phi_8. \tag{E10}$$

We note that, as $|f_2| < 1$, $|\phi_8| < 1$, and $|f_2| > |\phi_8|$, δ_2 and δ_8 satisfy $0 < \delta_a < 1$ ($a = 2, 8$).

Since δ_2 and δ_8 depend on x, it is difficult to solve Eqs. (E9) and (E10). However, Eq. (E5) becomes Eq. (E10) if we replace $3m^2/4$ with $3m^2(1 - \delta_2)/4$. Therefore, it is expected that the coherence length $\xi_{\max}$ obtained from Eq. (E10) is longer than $\xi_8 = 2\eta/\sqrt{3}m$. From the masses for the classical fields in Eq. (19), the corresponding penetration depth is $\lambda_8 = \sqrt{2}/\sqrt{3}m$. If we can use $\xi_{\max}$ and λ_8, the GL parameter becomes $\kappa = \lambda_8/\xi_{\max} < \lambda_8/\xi_8 = 1/\sqrt{2}\eta$. If $\eta \simeq 1$, we can expect type-I.

References

[1] G. Ripka, arXiv:hep-ph/0310102[Search inSPIRE].
[2] H. Sawayanagi, Prog. Theor. Exp Phys. **2017**, 113B02 (2017).
[3] H. Sawayanagi, Prog. Theor. Exp. Phys. **2019**, 033B03 (2019).
[4] D. Zwanziger, Phys. Rev. D **3**, 880 (1971).
[5] G. Curci and R. Ferrari, Phys. Lett. B **63**, 91 (1976).
[6] H. Sawayanagi, Phys. Rev. D **67**, 045002 (2003).
[7] H. Sawayanagi, Prog. Theor. Phys. **117**, 305 (2007).
[8] K. -I. Kondo and T. Shinohara, Phys. Lett. B **491**, 263 (2000).
[9] D. Dudal and H. Verschelde, J. Phys. A **36**, 8507 (2003).

[10] Z. F. Ezawa and A. Iwazaki, Phys. Rev. D **25**, 2681 (1982).
[11] H. Sawayanagi, Prog. Theor. Exp. Phys. **2018**, 093B01 (2018).
[12] T. Suzuki, Prog. Theor. Phys. **80**, 929 (1988).
[13] S. Maedan and T. Suzuki, Prog. Theor. Phys. **81**, 229 (1989).
[14] S. Sasaki, H. Suganuma, and H. Toki, Prog. Theor. Phys. **94**, 373 (1995).
[15] H. Suganuma, S. Sasaki, and H. Toki, Nucl. Phys. B **435**, 207 (1995).
[16] H. Sawayanagi, Prog. Theor. Exp. Phys. **2021**, 023B07 (2021).
[17] J. M. Cornwall, Phys. Rev. D **54**, 6527 (1996).
[18] J. Carlson, J. Kogut, and V. R. Pandharipande, Phys. Rev. D **27**, 233 (1983).
[19] C. Alexandrou, Ph. de Forcrand, and O. Jahn, Nucl. Phys. B (Proc. Suppl.) **119**, 667 (2003).
[20] V. G. Bornyakov et al., Phys. Rev. D **70**, 054506 (2004).
[21] N. Sakumichi and H. Suganuma, Phys. Rev. D **92**, 034511 (2015).
[22] Y. Koma and M. Koma, Phys. Rev. D **95**, 094513 (2017).
[23] Y. Koma et al., Phys. Rev. D **64**, 014015 (2001).
[24] H. B. Nielsen and P. Olesen, Nucl. Phys. B **61**, 45 (1973).
[25] K. -I. Kondo et al., Phys. Rep. **579**, 1 (2015).
[26] S. Nakajima, Introduction to Superconductivity(Baifukan, Tokyo, 1971) (in Japanese).